AD-A174 039 ADVANCED MARINE VEHICLES A REVIEW(U) ASSOCIATION OF 1/1
SCIENTISTS AND ENGINEERS OF THE NAVAL SEA SYSTEMS
COMMAND WASHINGTON DC M R BEBAR ET AL APR 86
UNCLASSIFIED F/G 13/10 NL

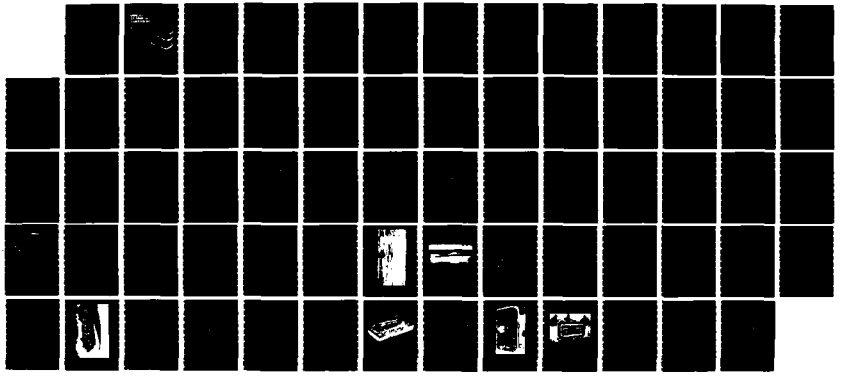

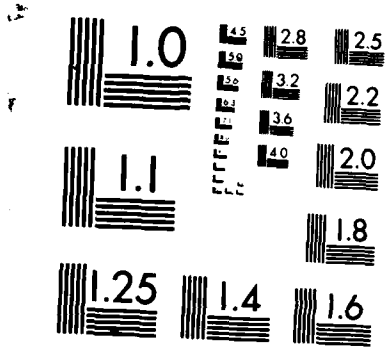

23RD ANNUAL TECHNICAL SYMPOSIUM 1986

"ASE's 40 YEARS OF ENGINEERING ADVANCEMENT"

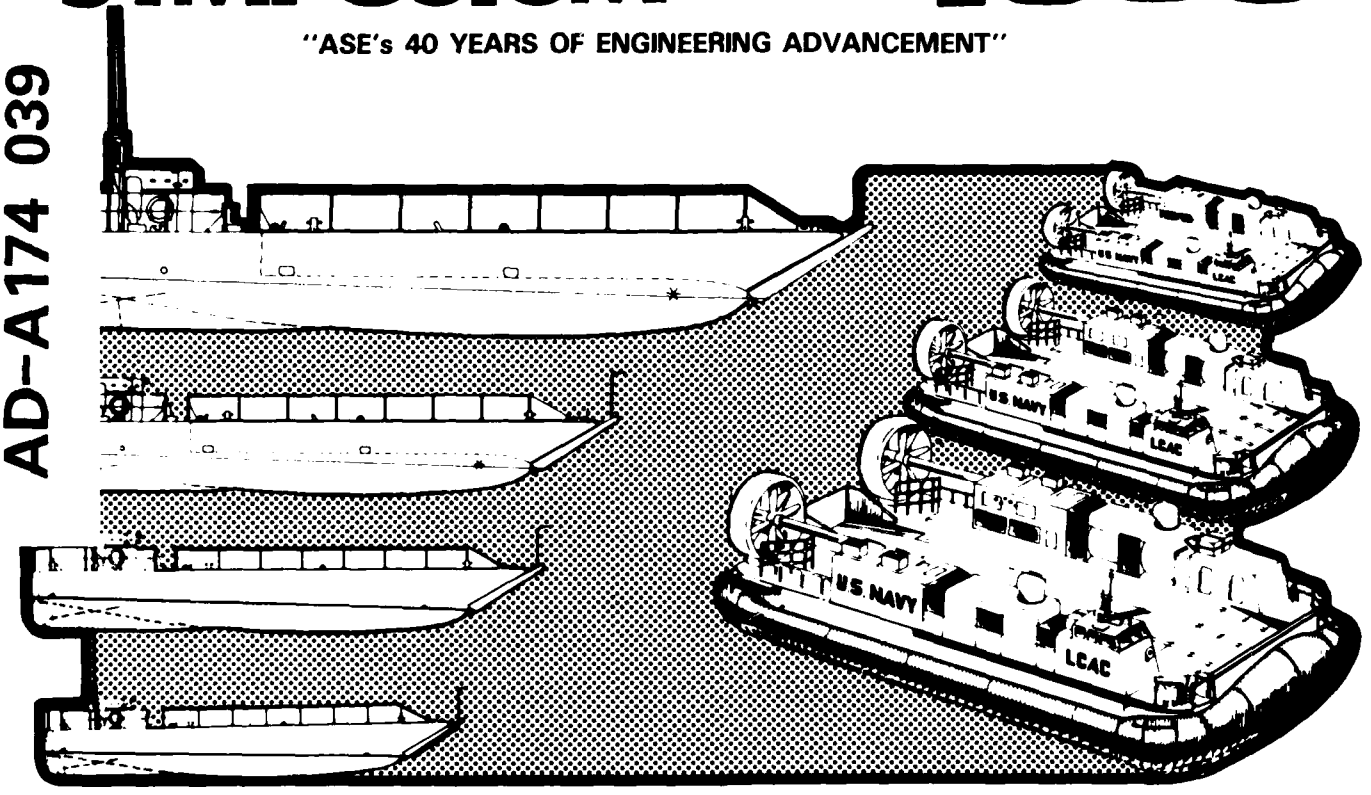

ADVANCED MARINE VEHICLES - A REVIEW

by: M. Bebar
Naval Architect

ASSOCIATION OF SCIENTISTS AND ENGINEERS OF THE NAVAL SEA SYSTEMS COMMAND • DEPARTMENT OF THE NAVY • WASHINGTON, D.C. 20362

ADVANCED MARINE VEHICLES

A REVIEW

Mark R. Bebar
Colen G. Kennell
William N. White

Naval Architects

Preliminary Design Division
Naval Sea Systems Command
(SEA 501)
Washington, D.C. 20362

and

David R. Lavis
Band, Lavis and Associates, Inc.
Severna Park, MD 21146

April 1986

The views expressed here are the personal opinions of the authors and are not necessarily the official views of the Department of Defense or of the Department of the Navy.

ADVANCED MARINE VEHICLES - A REVIEW

ABSTRACT

The purpose of this paper is to provide an overview of hull form design practices as applied by NAVSEA 501 in the design of hydrofoils, small waterplane area twin hulls (SWATH), surface effect ships (SES), and air cushion vehicles (ACV) for the U.S. Navy. General design considerations will be discussed in the context of specific examples of recent advanced vehicle hull form design. This paper was presented previously at the Workshop on Hull Form Design held at the Maritime Research Institute, Netherlands (MARIN), Wageningen, October 22-24, 1985.

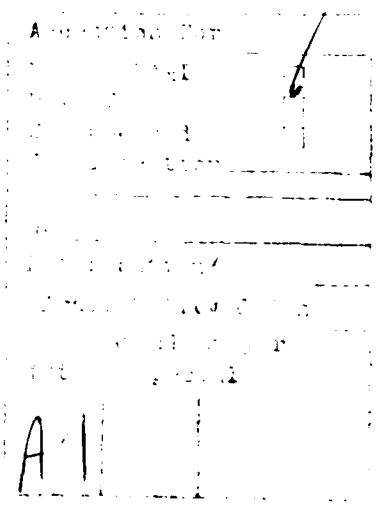

TABLE OF CONTENTS

TABLE OF CONTENTS

FIGURES

TABLE OF CONTENTS

FIGURES (cont'd)

TABLES

ACRONYMS

ACV	Air Cushion Vehicle
C_R	Residual Resistance Coefficient
DWL	Design Waterline
$\Delta/(.01L)^3$	Displacement-Length Ratio
EHP	Effective Horsepower
F_R	Froude Number
GML	Longitudinal Metacentric Height
GMT	Transverse Metacentric Height
IGV	Inlet Guide Vane
LBP	Length Between Perpendiculars
LCB	Longitudinal Center of Buoyancy
LCG	Longitudinal Center of Gravity
L/B	Length-to-Beam Ratio
L/D	Lift-to-Drag Ratio
RD	Rotating Diffuser
SES	Surface Effect Ship
SSP	Semi-Submerged Platform
SWATH	Small Waterplane Area Twin Hull
V	Velocity
V_{TO}	Takeoff Velocity

INTRODUCTION

The purpose of this paper is to provide an overview of hull form design practices as applied by NAVSEA 501 in the design of hydrofoils, small waterplane area twin hulls (SWATH), surface effect ships (SES), and air cushion vehicles (ACV) for the U.S. Navy. The general format which will be followed for each hull type will be a discussion of the general design considerations for that hull type in the context of one or two specific examples of recent hull form design. It is emphasized at the outset that this paper is based on U.S. Navy design experience and therefore does not necessarily reflect practices which would be applied in the commercial sector for these vehicle types. The preparation of this paper was funded under the U.S. Navy's Surface Ship Continuing Concept Formulation (CONFORM) Program.

SECTION I. HYDROFOIL

1.1 Introduction

It should be noted that, while the hydrofoil ship must satisfy requirements unique to the concept, the fulfillment of these requirements generally results in hull forms similar to traditional (monohull) naval ships and must therefore follow traditional naval architectural practices. The U.S. Navy's experience since the early 1960's has been almost exclusively with fully submerged foil configurations, based on considerations of crew and combat system performance in specified mission scenarios which have stressed high speed in moderate to high sea states. In contrast, most commercial applications of hydrofoils in the world have utilized the surface-piercing foil configuration, based on consideration of factors such as transit time, calm-moderate sea conditions, moderate speed, and economic factors. Fig. 1 depicts the two generic types of foil configurations. The discussion which follows will reflect USN experience with hull forms for hydrofoil ships with fully submerged foil configurations.

1.2 General Hull Form Considerations

1.2.1 Displacement-Length Ratio

The displacement-length ratio ($\Delta/(.01L)^3$) is one of the most important hull form parameters to be determined because, once it is selected, the overall hull proportions are established. In the interests of saving hull structural weight, there is a strong tendency to make the hull envelope as small as possible, consistent with requirements for internal volume and topside arrangements. This has, in the past, led to hydrofoil hulls which were relatively short and beamy. Table 1 shows values of displacement-length ratios for several hydrofoils built in the U.S.

Table 1. Hydrofoil Displacement-Length Ratios

Ship	Displacement (LT)	Length (FT)	Disp-Length Ratio
PGH-2	58	65.8	204
Jetfoil	115	78.7	236
PHM-1	237	118.1	144

The first two ships reflect an earlier trend which was to make the hull as small as possible. The PHM was designed from the outset with a lower displacement-length ratio, being more driven by the need for internal space than by hullborne performance. The original design displacement of the PHM was 218 metric tons, with a waterline length of 36 meters, producing a displacement-length ratio of 130 (English units). This was a significantly lower number than used up to that time. The decision to use a lower value has worked out well, producing a hull form which has the lowest overall resistance characteristics of any USN hydrofoil hull. A good starting point for selecting displacement-length ratio is around 150. To obtain a sense of the effect of displacement-length ratio on hull resistance, data for a series of hulls is presented in Fig. 2. The hull represented is the DTNSRDC Series 62, considered to be one of the best planing hulls from a calm water resistance standpoint. The hulls tested were of the same weight, geometrically similar, but with different length-beam ratios and thus produced a range of displacement-length ratios. Note that the low displacement-length ratio hulls are superior in resistance characteristics up to fairly high speeds. Beyond about 30 knots (full-scale), except for the most slender hull, all hulls have generally the same resistance.

1.2.2 Freeboard and Flare

Freeboard is a quantity which is less amenable to absolute determination than many others. There are several factors affecting freeboard, some more qualitative than quantitative. One quantitative number can be obtained by determining the margin line requirements due to compartment flooding. Other than this, the influences are internal vertical space within the hull and general seakeeping and seaworthiness characteristics. The latter attribute pertains primarily to freeboard at the bow, which directly relates to deck wetness in a seaway. NAVSEA developed a freeboard recommendation in the early 1970's based on past practice on patrol boats and cutters. This is depicted in Fig. 3, and was used for the first time in the PHM design. The tendency for slender bows in a hydrofoil ship caused by the aft LCB will require fullness above the waterline for good recovery following wave entry. PHM flare, which is quite significant, is considered marginal in shedding water and recovery during a "crash" landing in a seaway. Hull section shapes in the region of the bow flare should be concave so as to throw water away from the hull at the deck edge, normally the point of water separation. If this does not allow enough flare or fullness to be incorporated, a knuckle may be introduced, which will separate the water lower on the hull. Flare should be continued aft as far as possible from the bow along the hull sides, consistent with foil system retraction, which will be discussed later.

1.3 Hydrofoil-Unique Hull Form Design Considerations

1.3.1 Load Distribution

Most discussions on hydrofoil load distribution center on the distribution of lift in the foilborne mode between the forward and aft lift system arrays. The terms conventional (or airplane), tandem, and canard are used to classify hydrofoil ships by lift system distribution. Fig. 4 illustrates the generally accepted limits for each type. USN hydrofoil ships have successfully utilized both conventional and canard configurations, the most recent, PHM, utilizing the canard arrangement. Future larger hydrofoils with lesser

strut length to ship length ratios and higher foil span to ship beam ratios will tend to employ tandem distributions. The final lift system distribution choice involves overall arrangement and weight distribution considerations, including location of major machinery and combat system elements, foilborne hydrodynamics relative to dynamic stability and control, and wake (downwash) effects of the forward foil on the aft foil. Not often recognized, however, is the requirement of the hull form to match the selected vehicle load distribution with minimal changes in trim. The single hull form parameter which defines the solution is the location of the longitudinal center of buoyancy (LCB) for the displacement of interest. Fig. 5 illustrates typical values of LCB suitable for the various lift system distributions discussed above. For level trim hullborne, the LCB location must match the location of the longitudinal center of gravity (LCG). It should be noted that, in the case of designs with retractable foil systems, lowering the foils will move both the LCB and LCG of the total ship. For this reason, hullborne level trim conditions cannot, as a rule, be precisely satisfied for both foils up and foils down conditions, although experience has shown that acceptable values of trim can be obtained in most cases.

1.3.2 Foil System Retraction

All USN hydrofoil ships have had retractable lift systems. AGEH-1 and PGH-1, with conventional lift system distributions, had split forward foil/strut arrays which were retracted athwartships, and a single tail strut and foil pivoted over the transom in the fore and aft plane. The lift system elements on the PGH-1 retracted vertically into trunks, but remained wet. The PGH-2, with a canard distribution, had a mirror image of the PGH-1 retraction, with split aft arrays retracted athwartships and the single forward array pivoted over the bow. The PHM, with a canard arrangement, has a single foil aft supported by two struts in an inverted "Pi" configuration; the single inverted "T" forward strut and foil pivot up over the bow. Generally, each of these retraction schemes has imposed no severe requirement on the hull arrangements or distribution of hull volume, other than local shaping (notch on PHM aft, for example) of the hull to accommodate the retraction details.

Retraction arrangements for future larger hydrofoil ships will not be as readily achievable as on past designs. There are several reasons, but most are related to achieving higher hydrodynamic performance in both foilborne and hullborne modes. For a given foil loading, foil dimensions increase by the 1/2 power of displacement, while hull dimensions increase by the 1/3 power. Foil efficiency is increased with increases in the aspect ratio of the foil planform. Thus, as future vehicle size increases, foil dimensions relative to both hull dimensions and aspect ratio will increase, eliminating the possibility of split foil arrays or single strut and foil combinations.

1.3.3 Takeoff Hydrodynamic Performance

The hydrofoil hull in takeoff differs from the conventional planing hull in that, being constantly unloaded, it has no fixed design displacement, and is subjected to high hull trimming moments due to the position of the drag vector from the lift system and thrust vectors from the propulsion system, especially in the case of propeller propulsion. It rarely, if ever, achieves a positive attack angle of the aft underbody (necessary for the definition of planing) and, in general, it experiences maximum drag values at velocities other than those experienced in planing craft.

In 1964, Savitsky, Ref. 1, presented formulas for the lift, drag and trim of planing hulls. Hadler, Hubble, and Holling, of DTNSRDC, compared the results of model tests of Series 62 and 65 forms with the Savitsky predictions, suggesting the Savitsky formulas needed correction for non-prismatic hull forms. Such a correction was attempted by Blount and Fox, Ref. 2, particularly to improve the prediction of drag near the hump speed. Such formulations provide the basis for preliminary drag estimates and also assist interpolation between available model test results. Ultimately, model tests are made of any proposed USN design to provide the best possible basis for power estimates.

In order to estimate the minimum drag at the takeoff hump, it is necessary to know the hull drag over a range of displacements down essentially to zero. (There is even some evidence that, perhaps due to wave formation, the water adheres to the bottom and causes some drag after the keel is raised above the still water level.) Model tests of proposed USN hydrofoil hulls are tested over a wide range of displacement to accommodate this situation. With increasing ship size and essentially unchanged takeoff speed, the lift/drag ratio of the hull is improved. At some point, it becomes preferable to drive the ship up to foilborne speed without use of foil lift. This happens at the speed at which the hull drag-weight ratio becomes greater than the ratio of foil drag-due-to-lift increment divided by the foil lift increment. The drag of the struts and foils can be derived from estimates of the foilborne drag with an addition for the increased wetted length of the struts. At higher hullborne speeds, some thought must be given to carrying some lift on the foils, especially if flaps are used for lift control. Hull/strut interference may be significantly affected by the incorporation of fairings at the intersection. The design of an optimum configuration requires precise model tests. Since hydrofoil ships typically exhibit a maximum of drag at or near takeoff speed, careful attention must be given to control of the hump drag. The dashed curves in Fig. 6 show the drag in the foilborne mode down to the minimum speed at which sufficient lift can be developed by the foils to support the ship, and, below this speed, the drag of the ship in the hullborne mode with no lift generated by the foils. There is also shown, by a dot-dash curve, the drag in the range of foilborne speeds with the foils at such a depth that the hull is just clear of the water. It is evident from these curves that the foils are more efficient than the hull at the minimum foilborne speed, which suggests that the drag during takeoff can be reduced by carrying some of the ship weight on the foils. This is indeed the case and, by a suitable ship automatic controls program, the drag throughout the takeoff run may be made to follow the continuous curve shown.

To illustrate the relative contribution of the hull to the total hydrofoil drag during the takeoff transition, some typical cases will be shown based on actual hull model test data. This data resulted from a PHM candidate hull form model tested in 1971. The towing tank tests provide an adequate data base for valid prediction of hull drag and pitch for a considerable range of design displacements and loading conditions. The design displacement was 173 tons, with an LBP of 120 feet, yielding a displacement-length ratio of 100. Anticipated takeoff speed was 25 knots. Typical residuary resistance coefficients are shown in Fig. 7. These data are expanded and added to frictional drag for two illustrative hull sizes of 100 tons and 1,065 tons, Fig. 8 and Fig. 9, both for 25-knot takeoff

conditions. For the 1,065-ton ship, a higher takeoff speed of 35 knots was also considered, Fig. 10. A standard unloading with hull displacement proportional to takeoff speed squared,

$$\Delta_H = \Delta_D \left[1 - \left(\frac{V}{V_{TO}} \right)^2 \right] \qquad \text{Eq. (1)}$$

was used in this analysis. Fig. 11 compares the hull resistance per ton and corresponding lift-to-drag (L/D) ratios for the three examples.

For the 25-knot takeoff cases, the resistance per ton of the 100-ton craft is about twice that of the 1,065-ton ship. Comparing the 25-knot and 35-knot takeoff speed cases in Fig. 11 for the 1,065-ton displacement, hull resistance is similar up to about 23 knots, where hull L/D (approximately = 20) is greater than that to be expected from the foil system at this speed. This illustrates that, as hydrofoils grow in displacement and length, increasing takeoff speed has certain advantages, primarily if it is desirable to optimize the lift system hydrodynamic design for maximum foilborne speeds. Foil efficiency at takeoff speed can be compromised to achieve better maximum speed efficiency, and the transfer of lift from the hull to the lift system delayed in compensation. This can be accomplished because hull L/D ratios are a function of the Froude speed relationship while the foil system L/D ratios are a function of absolute velocity. Indeed, early historic concerns about getting "over the hump" at takeoff will diminish with increasing ship size.

The final concern is the effect of dynamic trim during takeoff. Because the hull can be subjected to wide variations in trimming moments due to the drag of lift system components (causing bow-down trim), differential lift from the forward and aft foils and acceleration thrust excursions (causing bow-up trim on propeller driven craft), it is desirable to provide hulls which are relatively insensitive in trim and drag variation to these effects. Analytically, the trimming moments are treated as hull static moments, providing a shift in the craft longitudinal center of gravity (LCG).

1.4 Hydrofoil Design Examples

Fig. 12 and Fig. 13 present the body plans and hull particulars for two hydrofoil designs of current interest to NAVSEA. Fig. 12 is the hull form baseline for a 786-ton ASW hydrofoil currently in the prefeasibility study stage for Special Working Group/6 (SWG/6) within NATO. The requirements for this ship call for high hullborne speed and range capabilities, resulting in a relatively slender hull form, with a tandem foil configuration. Fig. 13 is the current hull form baseline of the hydrofoil alternative for the Patrol Combatant Multi-Mission (PCM) which is a potential follow-on to the PHM in the 500 to 600-ton size range. Low hullborne speed requirements and the need for minimum cost result in a compact hull form for this design, which will incorporate a canard foil configuration. In addition to hydrofoils, SES (discussed in Section III of this paper) and high speed monohulls are under consideration for PCM, and a decision on the hull form is expected in the Spring of 1986. Ride quality in moderate to high sea states at high speeds will be a key decision factor in the PCM hull form selection process.

Both of these designs feature high deadrise sections forward, consistent with takeoff and high speed operations in high sea states, and full, moderate deadrise sections aft for satisfactory takeoff hydrodynamics and acceptable powering characteristics in the hullborne mode.

Both hull forms incorporate a "notch" aft, with vertical hull sides aft of the notch, in order to accommodate fully retractable aft foil systems. The PCM hydrofoil will utilize an inverted "T" foil/strut array forward, while the SWG/6 design will incorporate inverted "Pi" arrays forward and aft.

1.5 Concluding Remarks

The preceding paragraphs have briefly summarized some of the major factors considered in the design of hull forms for USN hydrofoil ships. Experience to date and that being obtained from the Navy's continuing operation of the PHM squadron in the Caribbean provide the information necessary for current NAVSEA efforts on the PCM and SWG/6 hydrofoil designs. The hydrofoil's seakeeping qualities in both the hullborne, foils down, and foilborne modes make it an attractive candidate for these and future U.S. Navy missions.

SECTION II. SMALL WATERPLANE AREA TWIN HULL (SWATH)

2.1 Introduction

The SWATH ship concept has been actively studied in the U.S. Navy for about 15 years. Analytic studies, model tests, and designs have been produced to assess the attributes and limitations of this hull form for a variety of naval missions. These studies have shown that the principal attribute of SWATH ships is superior seakeeping in rough seas while the principal limitation is a size/cost penalty relative to monohulls for equal payload capability. Other attributes have been identified which are expected to enhance performance of particular missions. For instance, the low motions at the bow of a SWATH ship coupled with the near absence of keel slamming and bubble sweepdown should enhance the performance of hull-mounted sonar arrays. Location of machinery self-noise sources in the cross-structure should further enhance sonar performance as well as reduce acoustic detectability.

The hull forms of USN SWATH designs currently being produced differ significantly from those produced in the early 1970's. The changes that have been introduced reflect advances in SWATH ship technology as well as design integration experience gained on successive designs. This section will describe the hull form geometry of a SWATH ship currently being designed for potential acquisition in the next decade. A frigate design has been selected for illustrative purposes since the frigate mission has been repeatedly studied throughout this time period. Hull form design techniques and concepts are similar for other missions. However, the hulls for these other mission designs will be different due to differences in requirements such as sustained speed, endurance, endurance speed, and mission equipment. Hull form features will be compared with earlier frigate designs to illustrate changes that have evolved. The motivation behind the hull form changes will also be discussed.

The underwater hull form of SWATH frigate designs produced in the early 1970's consisted of lower hulls that were simple bodies of revolution with

one or two struts per hull piercing the free surface. Fig. 14A and Fig. 14B show sketches of some of these early concepts. These designs reflect state-of-the-art SWATH hull form technology (resistance, propulsion, seakeeping, maneuvering) for that era as well as our ability to integrate machinery, propulsors, and sensors in a SWATH design.

Early SWATH frigate hull form designs rigorously adhered to the classic SWATH hull form definition as depicted in Fig. 14A and Fig. 14B. Such rigid thinking was due to the limits of our knowledge of the concept at the time the designs were produced. Experience gained through more detailed designs, analytic studies, and model tests has pushed back the boundaries in design space that define the SWATH ship. The success of these efforts has encouraged further assaults on the SWATH ship design constraints. Consequently, a number of the hull form features found in the current frigate design have not been validated by analytic studies or model tests. These designs are being used to lead SWATH research to produce the flexible, validated design tools required to design the next generation of frigates.

2.2 Discussion

Fig. 15 is a sketch of a SWATH frigate concept currently under development for potential acquisition in the 1990's. Hull form features that differ significantly from the earlier frigates have been included in this concept. Most of the features are reflected in the distribution of volume in the hulls, the section shape of the hulls, and the location of this volume relative to the design waterline. The most obvious change in hull form is the use of variations in diameter along the length of the hull. The earlier frigates used hulls consisting of a nose cone and a tail cone connected by a cylindrical mid-section. The mid-section on the current hull consists of a series of conical and cylindrical sections. The primary reason for using such a bulged hull (in particular, the large bulge amidships) is to reduce residual resistance. The principal reduction is realized for speeds between Froude No. 0.27-0.33. This speed range corresponds to endurance speeds for the frigates considered. Use of midship bulges alone generally reduces resistance at this "prismatic hump" while increasing resistance at higher speeds. Smaller bulges located near the forward and aft perpendiculars have been used to keep this high speed penalty within acceptable bounds. Interactions between the prismatic hump bulge and the high speed bulges have resulted in some compromises in performance at both endurance speed and maximum speed to achieve an acceptable design balance.

Use of the bulged hull results in a lower hull prismatic coefficient on the current frigate than those used on the older designs. Hull form parameters for the three concepts are tabulated in Table 2. Use of simple, non-bulged hulls restricts prismatic coefficient to values greater than 0.7 for realistic combinations of the nose and tail shapes used. Practical design considerations have resulted in the use of somewhat higher values in the older designs shown. The consequences of these hull volume distribution changes can be seen in the residual resistance coefficient curve (Fig. 16) and the effective horsepower (EHP) curve (Fig. 17) for the three designs.

The bulged hulls also provide more generous proportions at several locations along the hull for arranging machinery systems in the hulls. Propulsion motors can be located on the hull centerline with adequate

clearance on either side for access and maintenance. In general, oval sections provide more usable deck area for a given amount of hull volume than circular sections. These advantages are offset by the added cost associated with building the more complex hull shape.

The second major change in hull volume distribution is evident from the sections shown for the three concepts. The early designs used circular hull sections while the hull form currently being developed uses oval sections over most of the length of the hull. The oval sections must transition to circular sections at the stern to be compatible with the propellers. Such sections have been used to enhance seakeeping performance. Added mass of oval sections is greater than for circular sections leading to longer natural periods for heave, pitch, and roll. These increased natural periods lead to reduced motion excitation in operational sea states. Motion excitation at longer wave lengths is increased. This causes the designs to contour the longer waves and thereby reduce the frequency of water contact with the cross-structure. Ship motions at these increased natural periods are further improved by the increased damping of the oval sections. The oval sections also result in lower draft for a given hull centerline submergence. Draft reductions of about 12 percent have been achieved using oval hulls. The wetted area and shell area of a hull with oval sections are a few percent greater than in a circular hull for a fixed amount of hull sectional area. These increases lead to added frictional resistance and structural weight for hulls with oval sections.

Comparison of the non-dimensionalized hull centerline draft for the three designs in Table 2 shows that the hulls of the current frigate are somewhat closer to the design waterline than on the earlier designs. Deep hull submergence was considered necessary when the early designs were produced to keep resistance low and to assure that propellers would remain submerged in waves.

TABLE 2. Nondimensional SWATH Frigate Hull Form Parameters

	EARLY FRIGATES		CURRENT FRIGATE
	FIG 14A	FIG 14B	FIG 15
HULL PRISMATIC COEFFICIENT	.90	.90	.75
HULL CENTERLINE SUBMERGENCE	.41	.41	.32
WATERPLANE AREA COEFFICIENT	.94	.86	.78
STRUT LENGTH	3.1	4.1	4.2
STRUT THICKNESS	.15	.17	.17
LONGITUDINAL METACENTRIC HEIGHT (GML)	.23	1.43	.89
TRANSVERSE METACENTRIC HEIGHT (GMT)	.10	.05	.36

NOTE:
LENGTHS NONDIMENSIONALIZED BY $\sqrt[3]{\text{DISPLACED VOLUME}}$

These designs were produced without the benefit of a thorough understanding of the influence of hull form parameters on resistance characteristics. Since that time, more sophisticated resistance prediction computer programs have been developed and validated by a number of model tests. Resistance studies and designs produced using these programs have shown that deeply submerged hulls are not necessary to keep resistance at acceptably low levels. Several seakeeping model tests were made concurrent with these resistance studies. These tests showed that avoidance of propeller emergence in waves did not require such deep hull submergence. Consequently, designs produced since the early 1970's have had progressively lower hull submergences.

The shape of the hull centerline on the current frigate also differs from the earlier designs. Hull centerlines on the early designs were straight and at a constant submergence depth. The profile view in Fig. 15 shows that the hull centerline on the current frigate is segmented with some segments not parallel to the design waterline. The practical consequence of this kind of centerline is the flat keel that results for most of the length of the hull. This feature has been designed into the hulls to simplify building and dry-docking the ship.

Changes to strut characteristics have not been as dramatic as the changes to the hulls. Table 2 shows that struts have increased slightly in length as well as thickness. Strut length on the early designs was determined primarily by the length necessary to provide the minimum acceptable longitudinal metacentric height (GML). This parameter is still the principal factor in determining strut length although topside arrangement requirements are becoming progressively more important. Table 2 shows that the minimum GML judged acceptable has increased from the early designs. This increase has resulted from experience gained through analytic seakeeping studies and model tests. Designs with very low GML have been shown to have superior motions in head seas but decidedly inferior motions in following and stern-quartering seas at many speeds of interest. The very low wave encounter frequencies experienced at these speeds amplify the importance of the hydrostatic restoring force in the pitch equation. This term is proportional to GML. The increased GML designed into the current frigate results in a small amount of head sea performance degradation but significantly improved following sea performance.

Strut thickness in the current design has been increased to increase the tons-per-inch-immersion, improve access into the hulls, and increase transverse metacentric height (GMT) without increasing beam. Table 2 shows that the GMT designed into the current frigate is much larger than that of the earlier designs. Seakeeping tests of models with low GMT showed that such designs did not have satisfactory roll characteristics. A quasi-static heel angle was observed in addition to the expected roll motion. This undesirable characteristic has also been observed on the 200-ton SSP KAIMALINO. Models tested with increased GMT have been found to be free of this characteristic. Consequently, the higher GMT has been designed into the current frigate.

2.3 Concluding Remarks

Hull form design of SWATH ships has significantly changed since the early 1970's. This section has described the hull form differences between representative early designs and a current design, using frigate designs as an example. Many of the new hull form features included in the current design are extensions of current technology that cannot be precisely analyzed with current design tools. For example, the effect of the hull centerline changes on resistance cannot be accurately modeled analytically. Model tests are still required to measure these effects. Other features can only be analyzed in an approximate sense with today's tools. Examples of these are the resistance of hulls with oval sections and seakeeping of hulls with centerline changes. Experimental data to validate predicted performance is almost non-existent for such hulls. For instance, resistance and seakeeping data is available for only one hull form with oval sections. Consequently, some risk is associated with the use of these new hull form features. Research and development work must be done to demonstrate the feasibility of these hull form concepts prior to use in acquisition designs. This analytic, computational, and experimental effort is required to produce and validate the flexible design tools needed for the design of SWATH ships in the 1990's.

SECTION III. SURFACE EFFECT SHIP (SES)

3.1 Introduction

Surface Effect Ships trace their ancestry to the mid-1950's fully amphibious air cushion vehicles or hovercraft, originated by Sir Christopher Cockerell in Great Britain. In 1959, Ted Tattersall in the UK initiated development of the first Sidewall Hovercraft, later to be called an SES. At approximately the same time in the United States, a small team led by Alan Ford, then at the Naval Air Warfare Research Department of the Naval Air Development Center (NADC), invented a similar concept called the "Captured Air Bubble" vehicle which was a hovercraft with rigid sidewalls that penetrated the water surface and contained an air cushion between them when properly sealed fore and aft with bow and stern seals. Ford claimed that, despite the loss in amphibious capability due to the sidehulls, the design resulted in much higher lift-to-drag ratios due to the reduction in air leakage which the sidehulls provided.

Both men led teams that built the first two SES's. Tattersall, with the backing of William Denny and Bros., the licensees of Hovercraft Development Limited (HDL), built the first UK 70-ft manned model with a cushion length-to-beam ratio (L/B) of 7:1. This ship had a weight of 5 tons when powered with two 35-horsepower Mercury Outboards. Introduced on June 22, 1961 as the D.1 (see Fig. 18), the ship made 18 kts and lifted the cross-structure 1 foot above the surface. This first test craft was successful enough to lead to the building of the 70-passenger, 20-kt D.2 which went into experimental passenger service in 1963. HDL's pioneering efforts paid off; the direct descendant of those early pioneers is today known as Vosper Hovermarine Ltd., and this company has built more SES's than anyone in the free world.

In the United States, Alan Ford launched the XR-1 (Fig. 19) in May 1963. It was 50 ft long, weighed 10 tons and was propelled by a J-69 jet engine.

This 3.5 length-to-beam ratio SES achieved 60 kts with a more powerful J-85 jet engine. This original US SES has gone through eight major modifications over the years and is currently known as the XR1-E, some 22 years after it was originally built. It is constructed of steel, wood, and fiberglass.

These first two SES efforts set the tone for SES development in the two countries. Vosper Hovermarine concentrated on the commercial market, developing excellent cost-effectiveness with modest performance gains, while the U.S. SES concept developed into essentially a high performance military program designed to create an 80-kt Navy.

After these different paths were followed during most of the 1970's, and as the breadth of SES development spread, the first half of the 1980's has seen a consolidation of SES development. This is exemplified in the current close cooperation amongst NATO nations in the exploratory development of 500-1500-ton SES's for use as test craft and as corvettes. In the following discussion, the evaluation of the SES hull forms will show how the original goal of reducing the drag and power below that of an equivalent monohull has been achieved. The development of other aspects of the SES hull form of today which have been affected by stability, maneuverability, and machinery arrangement, and the integration of these features into the current SES state of the art design capability, will also be included.

3.2 Discussion

3.2.1 Cushionborne Performance

The most fundamental choice to be made about any SES is the cushion length-to-beam ratio. The proportion selected strongly affects the shape and magnitude of the cushion's wave-making drag. Fig. 20 illustrates this dramatically. There, cushion wave drag is plotted for different L/B versus a Froude number based on cushion area. Also along the abscissa are the referenced speed regimes for a 550-LT SES design candidate for the USN Patrol Craft Multimission (PCM) program. For this size vessel, a 7,000-square foot cushion area is required for a reasonable cushion density (P/ A) of 2.2. The selected L/B of 5.2 has a lower drag for all Froude numbers below 1.4. This particular L/B at the given displacement also yielded a wavemaking "bucket" between the so-called primary and secondary drag humps at a Froude number of 0.6. This characteristic bucket is highly desirable for sustained cruising with conventional monohull ships at their normal endurance (cruise) speed.

The utilization of these wavemaking buckets is a fundamental aspect of SES design and has been exploited from the first as evidenced by the L/B = 7 selected by the UK for their 18-20 kt original D.1 and the low L/B = 3.5 selected by the USN for its first high speed XR-1 which operated at Froude numbers, based on a cushion area, of up to 4 (see Fig. 20). This wavemaking drag characteristic generally means that high speed, smaller SES's, operating primarily at high speed (such as ferryboats), can be optimized with a low L/B configuration. On the other hand, SES's, which must operate over a variety of speeds such as do most military combatants, often find the high L/B geometry with its excellent low and moderate speed drag characteristics most attractive.

SES L/B ratios are not selected based entirely on wavemaking resistance. L/B also affects dynamic stability, and, to a lesser extent, static stability, arrangements, and structural bending moments. The two original SES both had basically simple flat plate sidehulls with the intent to minimize wetted surface and form drag. The D.1, due to its very shallow cushion depth and low speed capacity, had no stability problems. The XR-1 had a much higher cushion height-to-beam ratio and was much closer to a stability boundary. In fact, the craft as originally configured turned over during an early experiment. As a result, much more attention was put into designing adequate dynamic stability into SES from that time on. Fig. 21 illustrates some of the successful design approaches that have evolved. Initially, stability appendages were used, such as on the SES 100A which had low aspect ratio hydrofoils incorporated into the hull. They were of both fixed and variable geometry, depending on the need to minimize drag when they weren't in use. These approaches all worked very successfully. Another solution was to widen the cushion beam and also widen the sidehulls at the bottom to provide more restoring moment, thereby making the ships more stable. These latter changes were made to the XR-1 and worked well.

More sophisticated solutions evolved as time went on. They involved primarily adding deadrise to the sidehulls to provide dynamic lift without the high drag penalties associated with the box-shaped sidehulls that were initially added. Deadrise angles from about 30 to 45 degrees have been found to provide a good balance between sidehull drag and the required restoring roll moment. Recently, variable deadrise geometries have been found to minimize drag and maximize stability with a small penalty in construction.

Appendages are also still used for stability augmentation today. They have typically been integrated into the propulsion system with canted rudders, fins, partially submerged propellers, steerable propellers, waterjet steering nozzles etc., so that they serve both the functions of stability augmentation and of steering control. To continue with the PCM design as an example, it has, on the outboard sidehulls, 45-degree deadrise angles (Fig. 22) that extend up to the chine/spray rail located at the 2.5 ft waterline. This provides a 3.5 foot wide planing surface, creating positive dynamic roll moments in turns while still yielding a fine sidehull entrance angle to minimize drag and vertical accelerations from sidehull buoyancy contributions. Since the PCM performance envelope does not require an extremely high L/B ratio, the complexities of multiple deadrise angles are not needed in this case.

3.2.2 Hullborne Performance

Up until the end of the 1970's, hullborne performance was only considered in terms of very slow speeds such as those used for docking, stationkeeping, or in a failure mode. Addressing these conditions was very simple. The SES floats on its box-shaped cross-structure like a barge with two very long and effective sidehull keels. It makes a very stable, easily maneuverable configuration. The sidehull/keels dampen motions and minimize drift. This effect, coupled with the wide separation of dual propulsors, yields a highly maneuverable ship at speeds up to about 6-7 kts at which point the resistance becomes prohibitive.

This effect is fine for such SES's as ferryboats that spend the great majority of their time at high cushionborne speeds or at very low hullborne

speeds. For many other applications, such as the current PCM, however, there is a requirement to operate at 10-20 kt speeds a significant amount of the time. This issue was first raised seriously by the USN during the latter stages of the 3KSES (the 3,000-ton, 80-kt proposed demonstration USN SES frigate) program. To operate at 6-25 kt speeds for extended periods, the 3KSES program developed and demonstrated on three manned test craft the concept of partial cushion operation. The idea was to cut down the lift power to the minimum required to inflate the seals and just lift the cross-structure clear of the water. This eliminated the box structure drag present during normal hullborne operations. This partial cushion approach worked very successfully on the XR1D, the SES 100A, and the SES 100B. On all U.S. SES designs since then, it has become a standard operational mode for low speed operation. It was found that, typically, partial cushion operations could be sustained with only 10 percent of the normal fan power. However, it is still a compromise solution because of the increased skin friction drag of the partially submerged sidehulls added to the cushion wave drag and lift power penalties. Typically, 10 to 30 percent more power is required than for an equivalent displacement monohull operating at these low speeds, but, since less than 20 percent of the installed power is required at these speeds anyway, it is often a minor penalty to pay for the on-cushion SES high speed benefits. When an SES must cruise for long distances at low speeds, the efficiency directly translates into fuel costs and becomes significantly more important. Two solutions have been pursued--a cushionborne approach, and a hullborne approach.

The cushionborne approach resulted in the development of a new lift fan with the ability to create a totally new lift fan pressure versus flow curve as shown in Fig. 23. This fan, called the rotating diffuser (RD) fan, when coupled with Inlet Guide Vanes (IGV's), can create a totally flat pressure versus flow curve over a wide range of flows at high efficiency. This means that the reduced air flow requirements needed at low speed can now be achieved without a reduction in pressure. This reduces sidehull immersion and minimizes wetted surface drag. As a result, efficient low speed full-cushion operations should be possible. This concept has been built and land-base tested. Hopefully, at-sea demonstrations on the SES 200 will occur in the near future and provide additional operational data.

The desire to increase the hullborne speed capability of SES led to the incorporation of full displacement sidehulls jointly developed within NAVSEA by Mr. W. N. White and Bell Aerospace in New Orleans. The practical results are illustrated in Fig. 24 and were first demonstrated on the USN XR-5 and the first Bell Halter 110-ft demonstration SES. The basic change made was to take the vertical inner sidehull sides and angle them inboard to increase the sidehull thickness gradually from the keel to the cross-structure intersection. Since the inner sidehulls are out of the water when cushionborne, their changed geometry had negligible impact on the high speed performance. Enough buoyancy was gained on both the high L/B XR-5 and low L/B BH-110 with the new configuration angle to raise their cross-structures out of the water when hullborne. With these full displacement sidehulls, SES were transformed from barges to catamarans when hullborne.

The elimination of the cross-structure drag when the SES was hullborne more than doubled the economical hullborne operating speeds. Subsequent

refinement to these full displacement sidehulls have proceeded in this country, England, and France as typified by the SES 200, SWCM, and MSH in the U.S., the HM-5 and Deep Cushion SES in the U.K., and the Molenes in France. The most advanced SES's, such as the Deep Cushion and the Molenes, have totally integrated sidehulls, optimized simultaneously for both hullborne and cushionborne operations. The sidehulls below the cushionborne waterline are designed for cushionborne performance with the required deadrise and spray rails. Above the cushionborne waterline, the inner and outer sidehulls are shaped to minimize drag at the low hullborne design Froude numbers. In many ways, these structures resemble SWATH struts since they are designed typically to operate over the same speed envelopes.

Fig. 22 and Fig. 25 illustrate the baseline side hull geometry for the PCM. In the plan view, notice the asymmetry caused by the necessity to accommodate the bow and stern seals. This has not caused any increased drag in the SES's that have been built to date. In the cross section, the inner sidehull shape has been kept simpler than the more advanced European designs. Detailed cost versus performance trade-offs must await model tests to see if sufficient performance improvements would result from more sophisticated inner sidehull shaping. In any event, the current design configuration currently exceeds the hullborne range requirement by a factor of two with the baseline full displacement sidehulls. This improved low speed performance is in marked contrast to the 3KSES design that was cancelled 6 years ago partly because of its poor low speed efficiency.

Full displacement sidehulls have provided several additional benefits to the overall SES concept. First, as demonstrated on the SES 200 and HM-5, the sidehulls are now wide enough to be useful for machinery installation and other functions. This has had a major impact on propulsion plant design. The most important result has been the ability to incorporate conventional marine propellers or waterjets, gearboxes, shafting, and engine plants into SES sidehulls whereas they wouldn't fit in thin sidehulls. Significant cost savings and reliability improvements have resulted from the elimination of such complications as right angle drive gearboxes.

A second benefit from having a catamaran rather than a hullborne barge configuration was a significant reduction in structural loads due to slamming. A positive clearance of even as little as one foot can reduce the maximum load appreciably. Much greater load reductions are achieved when even more height is provided as in the PCM design. This configuration has a five foot clearance hullborne. On cushion, the 14-foot PCM cross structure clearance practically eliminates structural slamming in all but survival conditions, with significant wave heights approaching twice the cushion height as indicated by Fig. 26.

Recent U.S.N. studies have also explored the twin cushion SES, or SECAT, configuration which appears to offer certain advantages in terms of high speed, high sea state operations at small ship sizes. Ref. 3, 4, and 5 describe the SECAT concept in more detail.

3.3 Concluding Remarks

Significant progress has been made in the development of effective SES hull forms in the last 25 years, as typified by the 550-ton PCM design discussed here.

Performance improvements have been made through a balanced systems approach to SES hull form design. Hullborne vs. cushionborne, stability vs. maneuverability, structural loads vs. seakeeping, etc., have all been blended to achieve effective designs.

Based on the current worldwide commercial SES expansion, and the recent USN SES awards for the SWCM and MSH programs, the 25 years of hull form development is starting to pay significant dividends. With sufficient continued research and development effort, this momentum can continue to expand into the next decade.

IV. AIR CUSHION VEHICLES (ACV)

4.1 Introduction

In the last ten to fifteen years, significant contributions have been made toward developing a well-established discipline of amphibious Air Cushion Vehicle (ACV) design practice, comparable to that which is available for conventional ships. This has come about as a result of the wealth of experience gained by comparing and validating design procedures and design criteria against the very large data base of full-scale and model-scale information which has accumulated over a period of more than 25 years.

Foremost in this experience in the U.S. has been that provided by the U.S. Navy/Marine Corps Amphibious Assault Landing Craft Program, which produced the AALC JEFF(A) and JEFF(B) prototypes, and by the Amphibious Warfare and Strategic Sealift Program which produced the Landing Craft Air Cushion (LCAC) shown in Fig. 27 and which is now in quantity production.

This section of the paper provides an overview of this experience as it relates to the parameters which influence amphibious ACV hullform design.

Unlike the hull of a conventional ship, the hull structure of an ACV, under normal operating conditions, is seldom in contact with the water. The study of craft resistance, stability, and seakeeping normally associated with the hullform design of a conventional ship is, therefore, for an ACV, more appropriately associated with the study of ACV skirts.

For those not familiar with ACV technology, a description of the principle of air-cushion lift is given below. Included is a summary of the important considerations and constraints which dictate ACV geometry and the various options available to the designer. This is followed by a review of the state of the technology in ACV skirt design.

4.2 Hull Form Description, Options, and Constraints

An ACV is a surface vehicle which has its complete weight supported by a cushion of pressurized air. Air must be supplied continuously to this cushion to maintain the supporting pressure against the imperfect sealing of the cushion periphery formed by a flexible skirt, as illustrated schematically in Fig. 28.

The skirt is configured in such a way that, when inflated by the fan, it retains the cushion beneath the vehicle both when it is stationary and when it is underway. The function of the cushion is twofold: one is to minimize

resistance to forward motion, and the other is to provide a soft suspension for traversing rough seas or rough land surfaces. As a result of its geometric arrangement, the skirt also provides the major contribution to stability of the craft while it is on-cushion.

The pressure of the air cushion is very low. Typically, it is in the range of 0.2 to 0.7 psi for high-speed ACV's and of 0.7 to 1.2 psi for slow, heavy-lift hoverbarges. As a result, ACV's can operate over many surfaces which are normally denied to standard wheeled or tracked vehicles.

Lift power is proportional to the product of cushion pressure and cushion airflow rate. It is inversely proportional to the effiiciency with which the air can be delivered to the cushion. The power required to supply air to the cushion varies from approximately 5 h.p. per ton of displacement for slow hoverbarges to approximately 25 h.p. per ton for high-speed craft.

As the lift power is reduced, cushion airflow and the hovergap (Fig. 28) are also reduced, and vehicle drag is increased because of the increase in the drag of the skirt in contact with the surface. If the vehicle is to maintain speed, the thrust, and hence the propulsion power, must be increased. Lift and propulsion power are, therefore, normally traded, one against the other, until a minimum total power is found.

The optimum hovergap varies with the sea state or terrain being traversed and need not increase in proportion to vehicle size. Thus, as ACV's become larger, their lift systems become progressively more efficient (i.e., they need less lift power per unit vehicle weight).

ACV's can be designed for very high speeds. In calm conditions, the speed of an ACV can generally be higher than for other forms of marine transport. Usually, the thrust and installed propulsion power are determined by one or more of the following requirements:

- to climb an overland slope of a specified gradient,
- to traverse the hump in the overwater drag curve with a specified forward acceleration, and
- to cruise at a particular speed, above hump speed, in a specified sea state.

The characteristic shape of the resistance vs. craft speed curve for an ACV operating overwater is similar to curves for other high-speed marine vehicles, but unlike the curve for a conventional displacement craft. Fig. 29 shows predicted and experimentally determined drag for a typical ACV, the JEFF(B) experimental landing craft. Total drag for an air-propelled ACV such as JEFF(B) is comprised of 4 components: external aerodynamic drag, momentum drag of the lift system air, cushion wavemaking drag, and skirt or seal-system contact drag. Wavemaking drag reaches maximum values at the secondary and primary hump speeds, as shown in Fig. 29, and declines at high speeds. Hump drag increases with an increase in cushion pressure and a reduction in planform length-to-beam ratio. High speed drag increases also with increases in cushion pressure but decreases with a reduction in length-to-beam ratio. Skirt drag is a significant drag component, especially at high speeds in rough water. Aerodynamic drag is also a significant component of total drag

for the case shown because of the relatively blunt shape of the JEFF(B) hull and superstructure and the ambient wind condition (25-knot headwind in Fig. 29).

The manner in which ACV total resistance varies with changes in planform shape and size is only one factor among several which govern the selection of ACV geometry. Fig. 30 and Fig. 31 show, in carpet-plot form, the trade-off involved in total displacement and power for an ACV concept required to carry nearly three times the payload of the JEFF(B). The performance required was to cruise at 40 knots in Sea State 2. Fig. 30 shows results for craft propelled by airscrews and Fig. 31 for craft propelled by marine screws. For the airscrew-propelled craft, the selection of length and beam which results in minimum total power is well defined. In both figures, the extent to which length and beam can be changed without appreciably changing this power is shown by the shaded area on the upper plot of each figure.

Maneuvering control can be achieved by rudders in the propeller slipstream, by airjets issuing either from side ports (i.e., puff ports) or from swivelling nozzles fed from the lift-air supply fans, or by differential propeller thrust. Air propellers are sometimes pylon-mounted with freedom to rotate in azimuth and often have controllable- and reversible-pitch blades for additional control. Craft trim can be controlled by the transfer of fuel, by aircraft-type elevators placed in the propeller slipstream, or by a skirt shift, or lift, mechanism which controls the location of the skirt hemline relative to the hull. Often a combination of these maneuvering and trim control methods is used.

The designer usually has considerable freedom of choice in the selection of craft layout. This is a consequence, primarily, of the low cushion pressure and the very large planform area per unit displacement available for payload, machin-ery, and other essential accommodations and equipment. For example, the ratio of payload deck area to overall planform area for a single deck ACV is typically in the range of 0.4 to 0.85. Also, the beam of an ACV is generally half its length or more, thus providing additional flexibility for different arrangements. Fortunately, the ratio of disposable load (i.e., the payload plus fuel load) to all-up weight of an ACV can also be high, usually over 0.5. Therefore, high payload area and weight, for an ACV, go hand-in-hand. Although a high disposable load fraction is desirable, it can usually be achieved only by using very lightweight, and hence expensive, hull structure and propulsion systems.

A typical ACV is shown in Fig. 32. Its hull is a simple aluminum-alloy raft, the upper side of which forms a cargo deck. The machinery is arranged in the two superstructures on either wide of the cargo deck. In this configuration, each of the four propulsors is powered separately by a single gas-turbine engine, and the four lift fans on each side are powered by two more engines (six in all). Steering is provided by rotating the ducted airscrews on their pylons about vertical axes or by differential control of propeller-blade pitch.

The wide beam, raft-like hull of an ACV provides considerable buoyancy and intact stability when the craft is off-cushion over water. Watertight subdivisions internally provide stability for the damaged case, and landing pads or rails are located beneath the hull for parking on land.

The overall geometry of an ACV is often limited by considerations of its own outer envelope (as in the case of the LCAC, which must fit inside the well decks of existing landing ships), and/or considerations of the size and type of the payload that it must carry (buses, automobiles, and trailers in the case of the SR.N4; battle tanks, USMC vehicles, and weapons in the case of the LCAC). The structure usually has a simple, box-like form which lends itself to modularization for ease of transportation.

4.3 Skirt Design

4.3.1 Skirt Configurations

By far the most successful and widely used skirt configuration has been the bag/finger skirt which was first developed in the United Kingdom. The arrangement was used for the JEFF(B) and LCAC. It is featured in Fig. 27 and Fig. 34 and is illustrated in Fig. 28 and Fig. 33.

For both skirt designs, the highly compliant fingers or cells provide a responsive, low-drag cushion seal, while the bag acts as an air-distribution duct and provides increased restoring moments at large pitch or roll attitudes. Additionally, these skirts provide a high level of redundancy in that the failure of individual fingers or cells is largely compensated for by expansion of the adjacent units.

For bag/finger skirt systems, the cushion plenum is normally subdivided by stability seals to increase roll or pitch stiffness. Most commonly, this is achieved with a longitudinal "keel" on the centerline, and a lateral seal close to amidship as shown in Fig. 33 and Fig. 34. This arrangement results in three or four, approximately rectangular, cushion compartments. Frequently, the forward section of the keel is omitted to save cost and weight, at the expense of some roll stiffness. For the loop-pericell skirt (Fig. 35), stability seals have been found to be unnecessary and are omitted since they are difficult to inspect and maintain.

Alternative skirt configurations have found limited application to date. Some of these are summarized below:

- All-fingered skirts with no bag are frequently used for low-speed, heavy-lift platforms, and on small recreational ACV's. The principal advantages of this arrangement are simplicity and ease of maintenance.

- The French cell-type skirts offer high initial stability at the expense of drag and complexity in the air distribution system within the hard structure.

- Single or multiple lobe-bag skirts have been used as stern seals on both ACV and SES, but are now only found on SES configurations. Some small recreational vehicles have used single bags around the entire periphery, but this arrangement has proved less successful than fingers or bag/finger skirts.

4.3.2 Design Factors

Skirt Depth:

Skirt depth, hence buoyancy tank clearance (Fig. 28), is typically 20% of the cushion beam or less, to ensure adequate roll stability when underway.

The depth of the skirt is also limited by pitch stability requirements, particularly with respect to plow-in, as discussed later. For a tapered skirt configuration, where the clearance of the bow is greater by some 25 percent than the clearance at the stern, it appears that stern clearance is the critical dimension. The main advantage of a deeper skirt is improved obstacle and wave clearance, but the ability to utilize this clearance is highly dependent on the pitch characteristics of the vehicle. Excessive pitching of an ACV, as it crosses a series of waves, can cancel the benefit from the increased clearance height. In some military applications, the overall height of the ACV will be important. For example, in the case of the LCAC, there is a requirement for operating in the well-decks of dock landing ships. A secondary factor in the selection of skirt height is the total drag of the vehicle; while hydrodynamic drag is most significant, the aerodynamic drag of an ACV, such as the JEFF(B), will increase at a rate of 450 pounds per foot of skirt depth when traveling at 50 knots into a 25-knot headwind.

Side Loop Geometry:

Fig. 36 compares the geometry of the side skirts used on the JEFF(A) and JEFF(B). The support loop in each case was included for the following reasons:

- o Increased cushion area for a given hardstructure beam
- o Acts as an impact absorber
- o Effectively increases cushion height at the sides, bow, and stern by a factor of approximately 1.5. (In conjunction with deadrise on the hull bottom, the area of bottom over which the cushion height is increased is in excess of 50% in the case of the JEFF(A))
- o Provides an efficient method of distributing lift air to the respective groups of cells/fingers. Therefore, a minimum of ducting is required within the hull structure.

The loop also provides compliance to wave action analogous to that of a secondary suspension system. This is advantageous from the standpoint of ride. This additional degree of freedom is limited, however, by stability considerations, since the loop also helps to minimize skirt horizontal deformation in rough water or during a plow-in. The skirt system must also be designed to be free of dynamic instabilities such as skirt bounce under all operating conditions.

Mathematical model studies have indicated that it is possible to avoid skirt bounce by careful selection of design pressures. High pressure ratio, however, increases the power demand on the lift fan with a corresponding reduction in efficiency. In practice, to avoid excessive power loss, anti-vibration webs are installed within the skirt bag to allow operation in the (otherwise) unstable region.

No attempt was made to incorporate anti-bounce webs into the JEFF(A) pericell skirt design, since the bounce characteristic had not been evident in model tests. During early full-scale tether tests, however, a very pronounced skirt bounce behavior was experienced. Although designs for an anti-bounce web were explored, the phenomenon was eliminated (at all fan speeds) with the introduction of the JEFF(A) spray skirt.

On the JEFF(B), the side skirt was designed on the basis of unrestrained two-dimensional equilibrium, but vertical restraint was added by installing an anti-bounce web running the length of the bag. This allowed swinging motion in the vertical plane, but restricted the bounce and skirt depth change with fluctuating bag pressure.

Bow Loop Geometry:

A bow skirt should respond to the waves, but not collapse or tuck-under sufficiently to cause the craft to plow-in. In the case of the plow-in, the basic aim is to prevent the skirt on the leading side of the craft (which might be the bow, or one of the sides, of the craft) from distorting appreciably, as a result of water contact drag, and thereby moving inboard and under the craft with a consequent loss in cushion area and restoring moment. Increasing the skirt resistance to deformation and tuck-under is achieved by choice of inflated-loop radius, loop pressure, and location of attachments to the hard structure. Several design approaches are available to meet these requirements. First, the shape of the bow loop in planform is curved or bowed out as much as possible (to create a three-dimensional effect) within the limits of any craft-length restrictions. This creates additional longitudinal stresses in the bag, which in turn leads to a stiffening effect under bag deformation. Next, the outer attachment of the loop can be raised as far as possible to increase the outer loop radius and the hoop tension and thereby reduce the tendency for tuck-under or collapse during wave contact. This has been achieved to a somewhat greater extent for the JEFF(A) bow seal as compared to the JEFF(B), illustrated in Fig. 37.

Fig. 37 also shows the JEFF(A) bow loop to be considerably more shallow than the JEFF(B) bow loop with the cell-to-loop attachment point σ well aft of the upper attachment point τ, unlike the situation for the JEFF(B) skirt. This arrangement on the JEFF (A) was found (during model tests) to be more resistant to collapse. The larger bow loop on the JEFF(B) provides greater protection to the structure during wave slamming and generates a greater upward thrust in all but the most severe sea states.

A third approach is to introduce into the bow skirt a vertical anti-plow diaphragm between the outer finger attachment and the hard structure. This acts in two ways; the lower portion of the loop and the fingers are restricted to move in a radius about the hard structure attachment of the diaphragm, which restricts unwanted downward motion of the skirt; and, by running the diaphragm out into the side skirt, an enclosed area, or secondary bag, is formed. Non-return flaps in the diaphragm enable equal pressures to be generated in both portions of the loop under normal conditions, but any rearward motion, or collapse under wave loads, decreases the volume of the forward compartment, closes the non-return flaps, and raises the pressure. This results in increased tensions in the outer loop of the bag which in turn increases its resistance to horizontal skirt deflection.

Stern Loop Geometry:

It is generally recognized that stern skirts should be intentionally more sensitive to lifting forces and pressure changes than the bow and side skirts, since compliance is required to allow effective contouring of the waves for efficient cushion sealing and to reduce drag and wear loads.

Finger and Cell Geometry:

Exterior Angle (α)

The exterior α angle (see Fig. 37), between the water surface and the external face of the cell or finger, can greatly affect craft heave, roll, and pitch stiffness. The smaller the angle α , the greater the stiffness. For fixed loop attachment locations, however, a reduction in the angle decreases the cushion area.

Also, at small exterior angles, there is a tendency to increase water contact wetted length; therefore, there is an increase in drag plus a greater tendency to scoop when the fingers are deflected by waves. At large angles, the resulting increase in cushion area is offset by slower finger recovery after deflection and increased difficulty in providing a practical configuration for long support webs. For open fingers at the bow and stern sides, approximately 45-50° is considered to be the optimum angle for α . For pericells, α can be somewhat larger due to the greater inherent stability offered by cell compartmentation. For the JEFF(B) (at α = 50°), cushion area has been conserved by the introduction of an apron and box finger design as illustrated in Fig. 28.

Interior Angle (β)

The included angle β (see Fig. 37), formed by the outboard side of the pericell or finger and a line from the inboard attachment to the tip of the finger or pericell, should preferably be 90° to generate a satisfactory geometry which will inflate properly to the desired configuration. Normal cushion pressure acting on the finger's or cell's surfaces generates a load for cell tension in the semi-cylindrical outer face. This tension is supported by the finger or cell webs which are in turn attached to the hull or primary loop. As the included angle (β) is allowed to fall below 90°, the section of the finger or cell that is between the tip and the 90° intersection is no longer supported in direct tension. It therefore has to rely for stability on shear resistance from the elastomeric coatings, plus a degree of interlockings from the loaded warp and fill threads. A form of instability occurs when the tension loads can no longer be supported in this fashion and the lower unstable finger area is free to extend outwards. Finger/cells with a tip angle in the range of 80-90° will, however, perform satisfactorily if fabric stiffness and/or shear resistance in the lower finger area are adequate.

Finger and Cell Depth:

The ratio (expressed in terms of percent) of finger (or cell) depth to cushion depth can greatly affect seakeeping and obstacle negotiation. Increasing the depth of the finger reduces the rough water drag, but with a

penalty of reduced stability and, generally, reduced cushion area. Originally, one of the objectives of selecting a combination of bag and secondary skirt was to provide replaceable sections in the area subjected to the highest wear and abrasive action.

Early bag/finger designs used a 30% finger-to-cushion depth ratio; however, the bag was often in contact with green water while the craft was operating over waves. Since then, there has been a steady growth in finger depth percentage, and current skirt designs for most craft have finger depths from 50-70%.

Finger Depth-to-Width Ratio:

A depth-to-width ratio of approximately 1.5 has been established for open finger segments based on model test and full-scale development. There is evidence that relatively wide fingers or cells employed as side skirts are more susceptible to scooping loads. This is attributed to the larger hoop tensions and vertical resistance of wider fingers or cells. On the other hand, very narrow fingers or cells suffer from poor recovery and temporary hang-ups in conditions where large deflections occur. The general trend has been toward deeper and relatively wide fingers. As a general rule, pericells can be wider than open fingers with depth-to-width ratios of 1 to 1.5.

4.4 Concluding Remarks

This section has reviewed the options available and constraints imposed on ACV hull form design. In particular, several of the most important features of ACV skirt design have been identified. With few exceptions, ACV hull form design technologies are mature and we are now reaping the legacy of this as we enter an era of renewed ACV activity in the United States. The two transportation companies of U.S. Army LACV-30 lighters at Fort Story, Virginia will soon be increased to a total of 26 craft; the first in a fleet of over 90 Navy assault landing craft, LCAC's, are undergoing trials at Panama City, Florida, and the U.S. Army plans to procure a new family of heavy-lift hoverbarges, designated the LAMP-H. With the expected rapid growth in experience gained from such programs of ACV construction and operation, we anticipate a continued improvement in the technology base which will ensure the future growth in the use of these versatile craft.

REFERENCES

1. "Hydrodynamic Design of Planing Hulls," Savitsky, D., Marine Technology, Vol. I, No. 1, Oct. 1964, pp. 71-95.

2. "Small Craft Power Prediction," Blount, D.L. and Fox, D.L., Marine Technology, Vol. 13, No. 1, Jan. 1976, pp. 14-45.

3. "The Surface Effect Catamaran--A Sea Capable Small Ship," Wilson, F.W. and Viars, P.R., AIAA 6th Marine Systems Conference, Sept. 1981.

4. "Feasibility Design for a Surface Effect Catamaran Corvette Escort," Wilson, F.W. and Viars, P.R. AIAA/SNAME/ASNE 7th Marine Systems Conference, Feb. 1983.

5. "The Surface Effect Catamaran--Progress in the Concept Assessment," Wilson, F.W., Viars, P.R. and Adams, J.D., ASNE Journal, Volume 95, No. 3, May 1983.

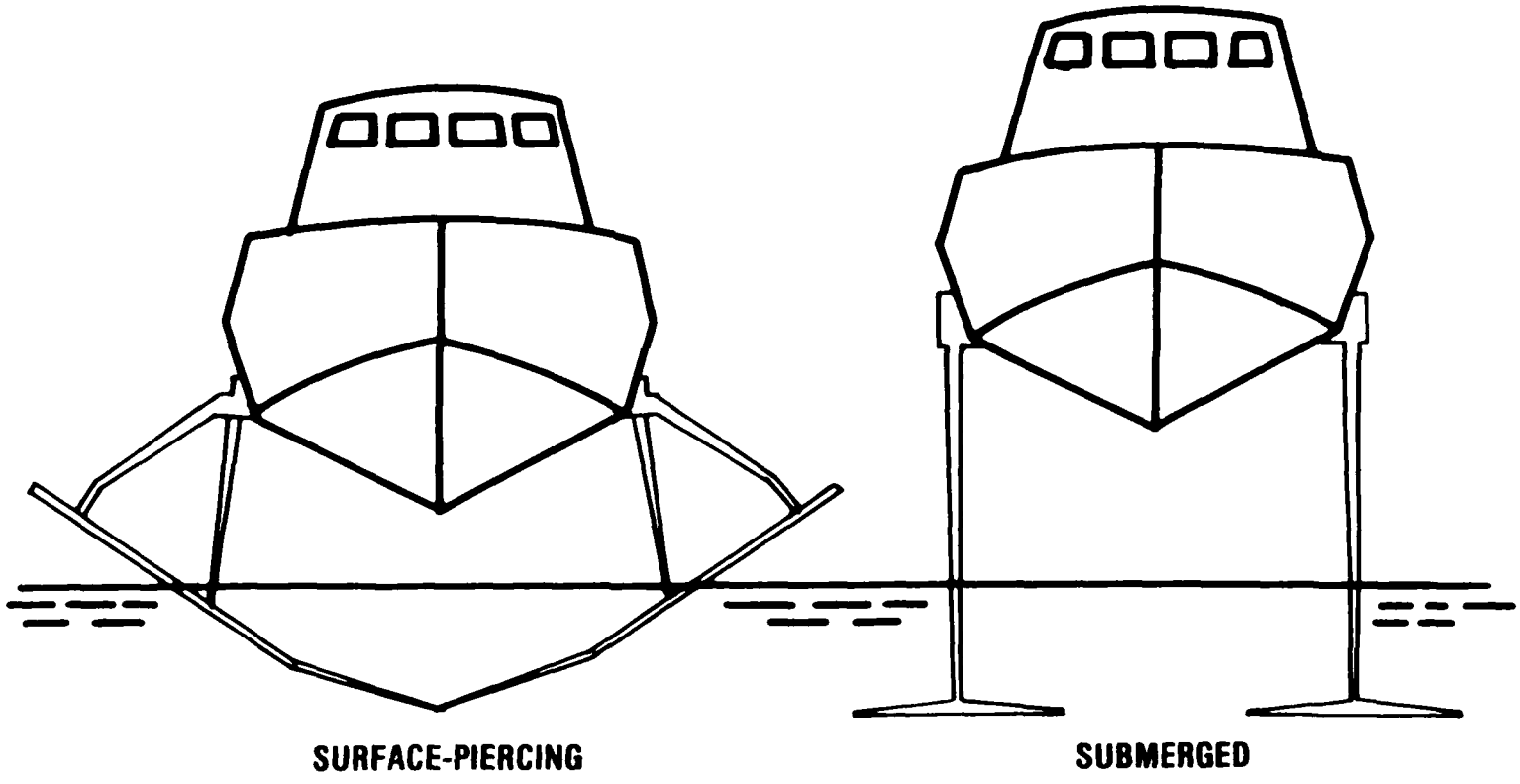

Figure 1. Hydrofoil Ship Foil System Types

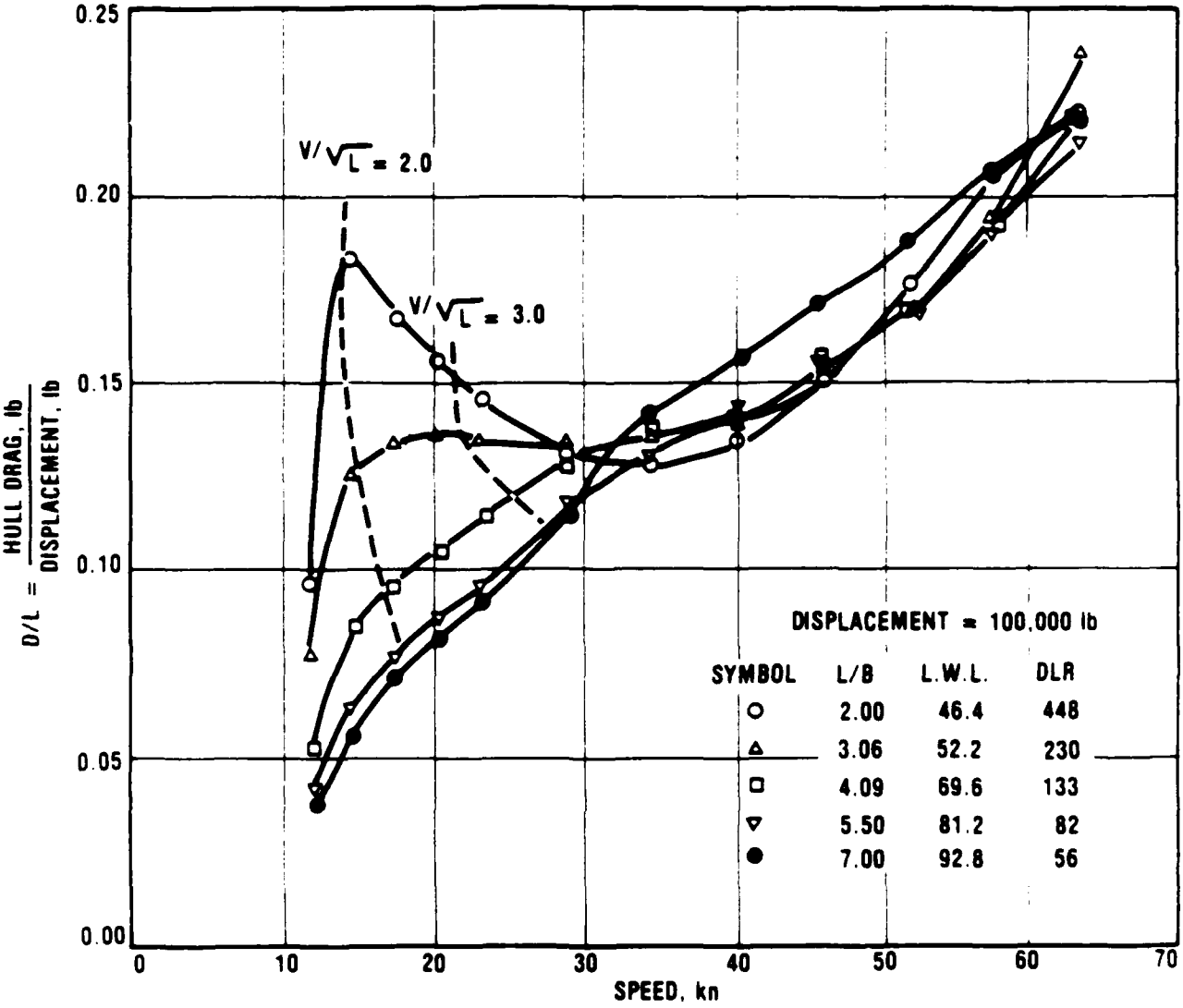

Figure 2. Series 62 Planing Hulls - Effect of Ship Displacement - Length Ratio on Ship Drag

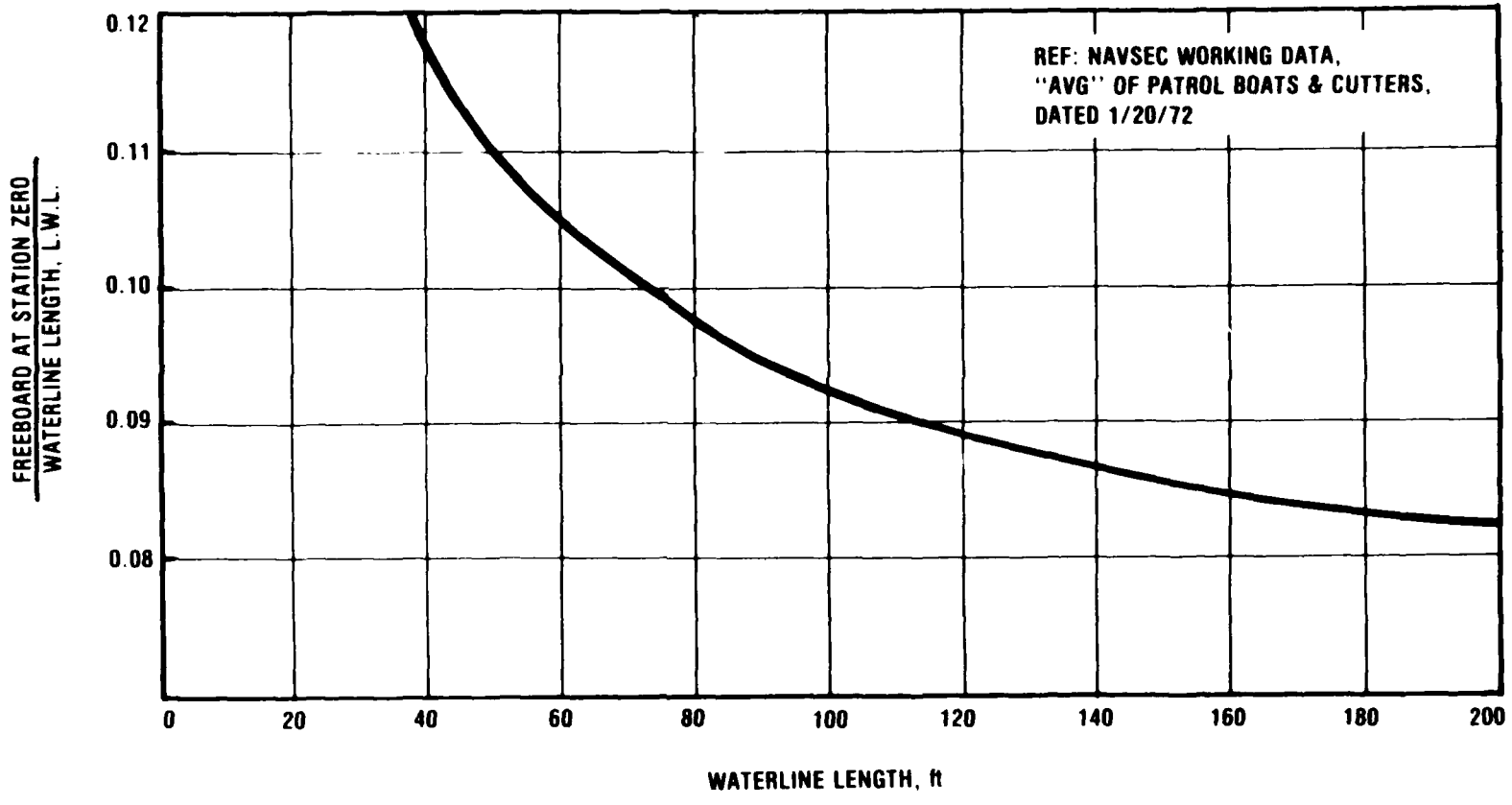

Figure 3. Freeboard Recommendation

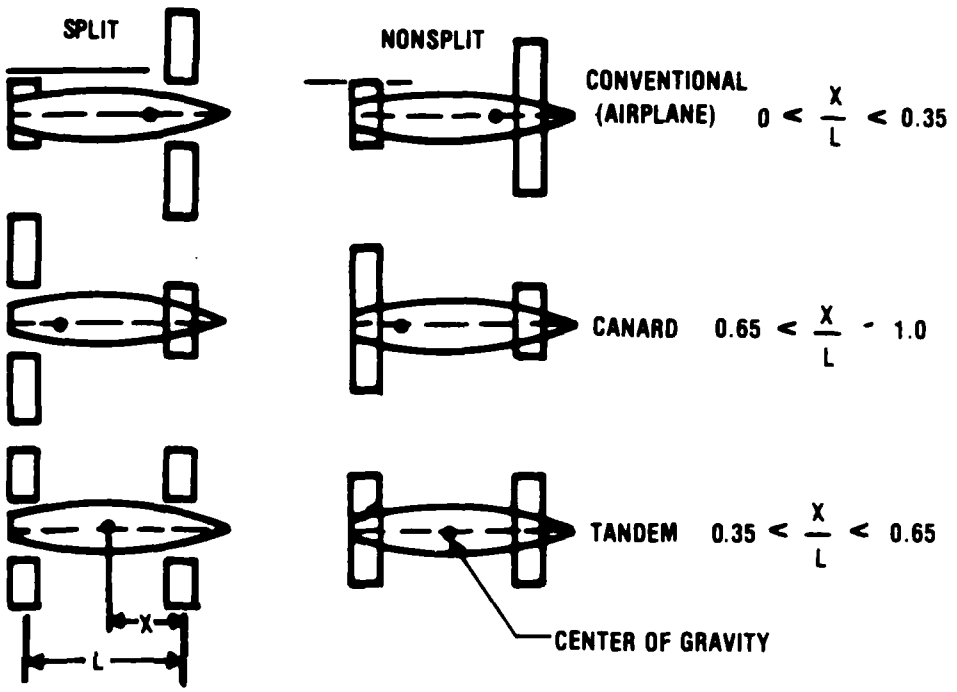

Figure 4. Definition of Foil Area Distribution

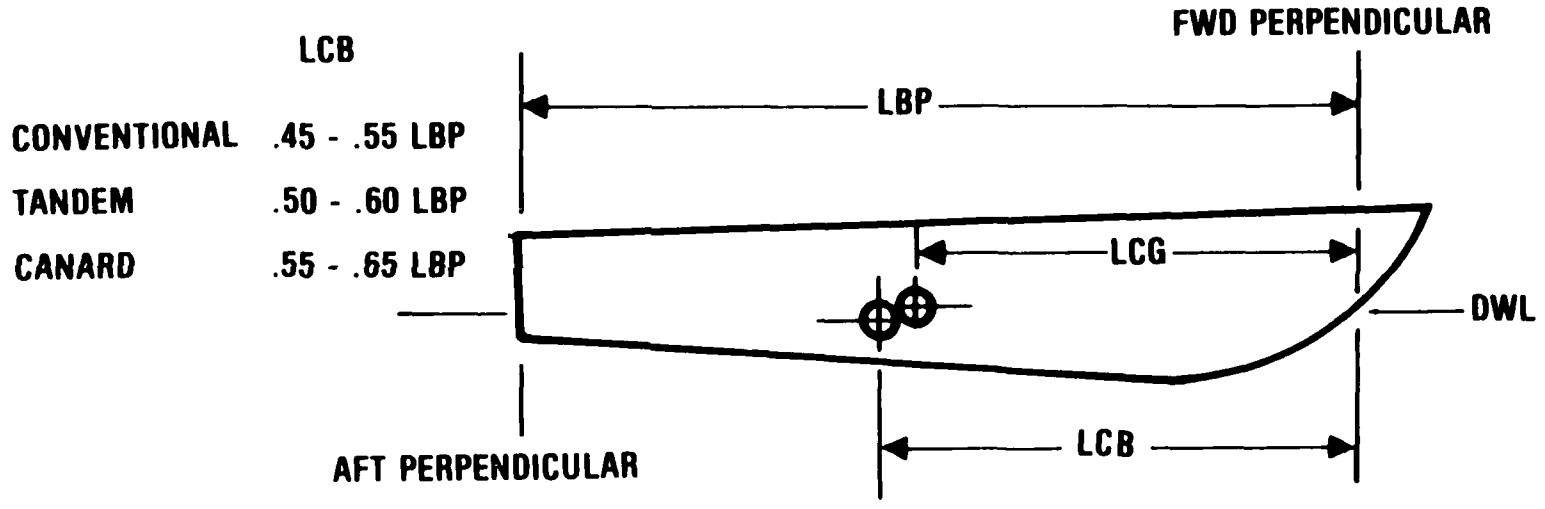

Figure 5. Typical LCB Locations for Hydrofoil Craft

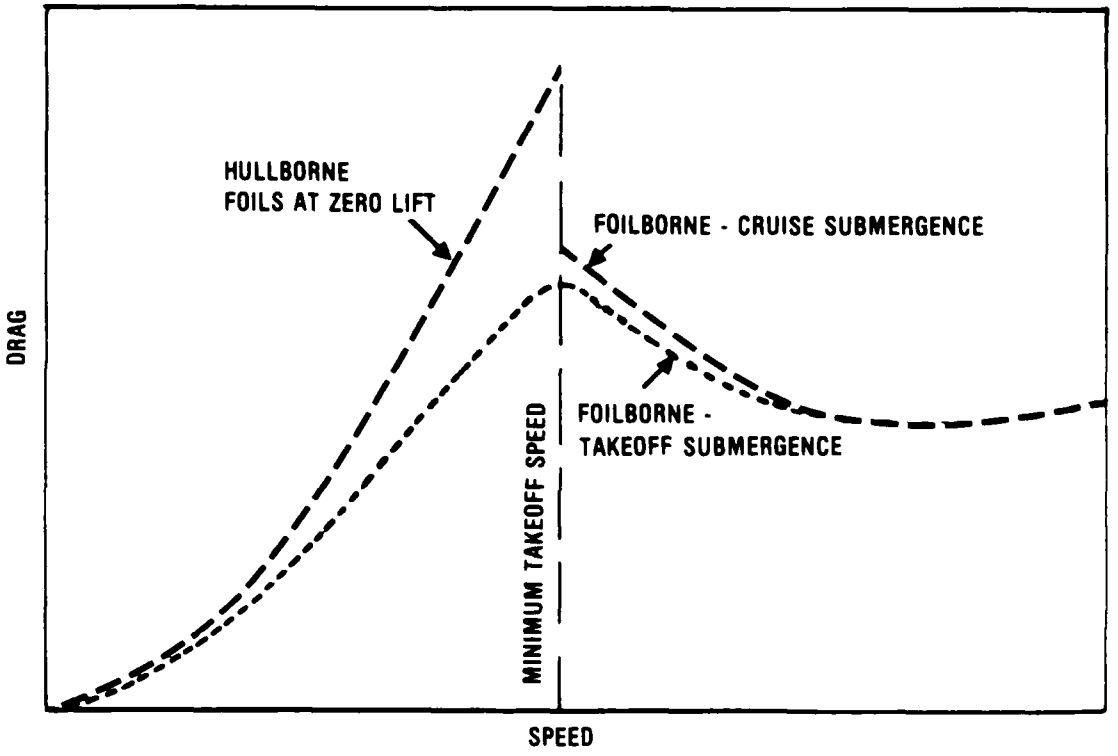

Figure 6. Hydrofoil Takeoff Drag

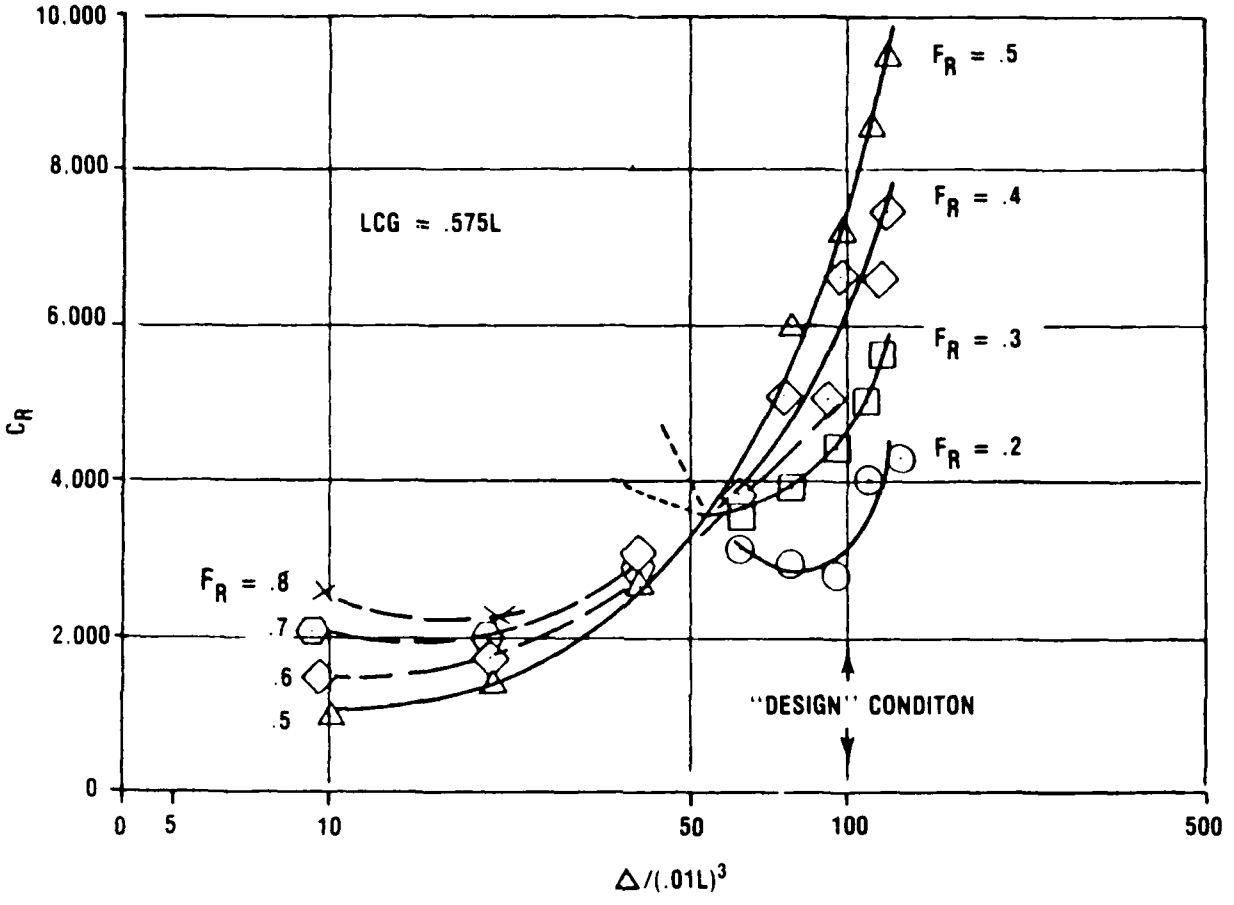

Figure 7. Typical Residuary Resistance Coefficients

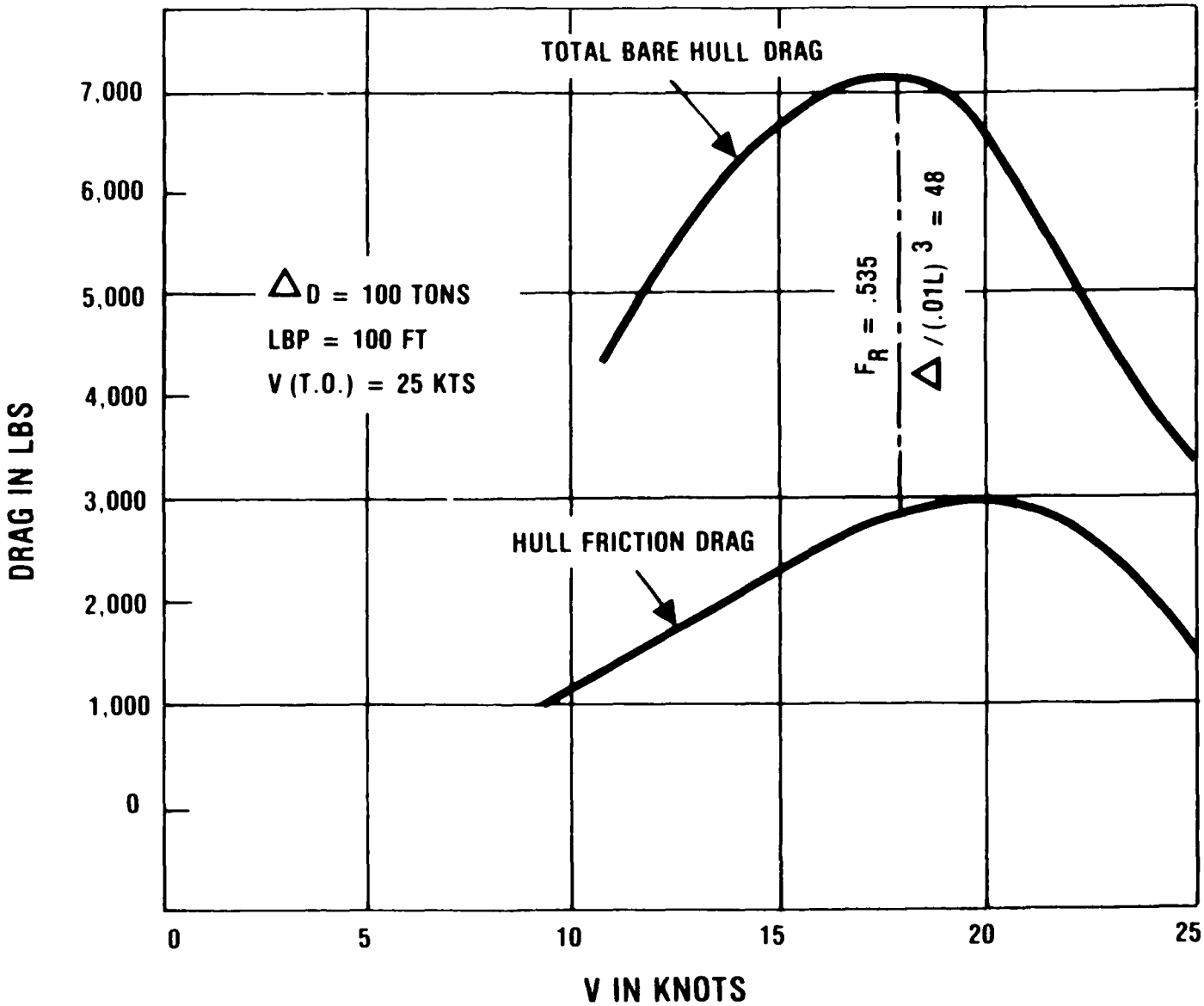

Figure 8. Bare Hull Drag for 100-Ton, 25-Knot Takeoff Speed Design

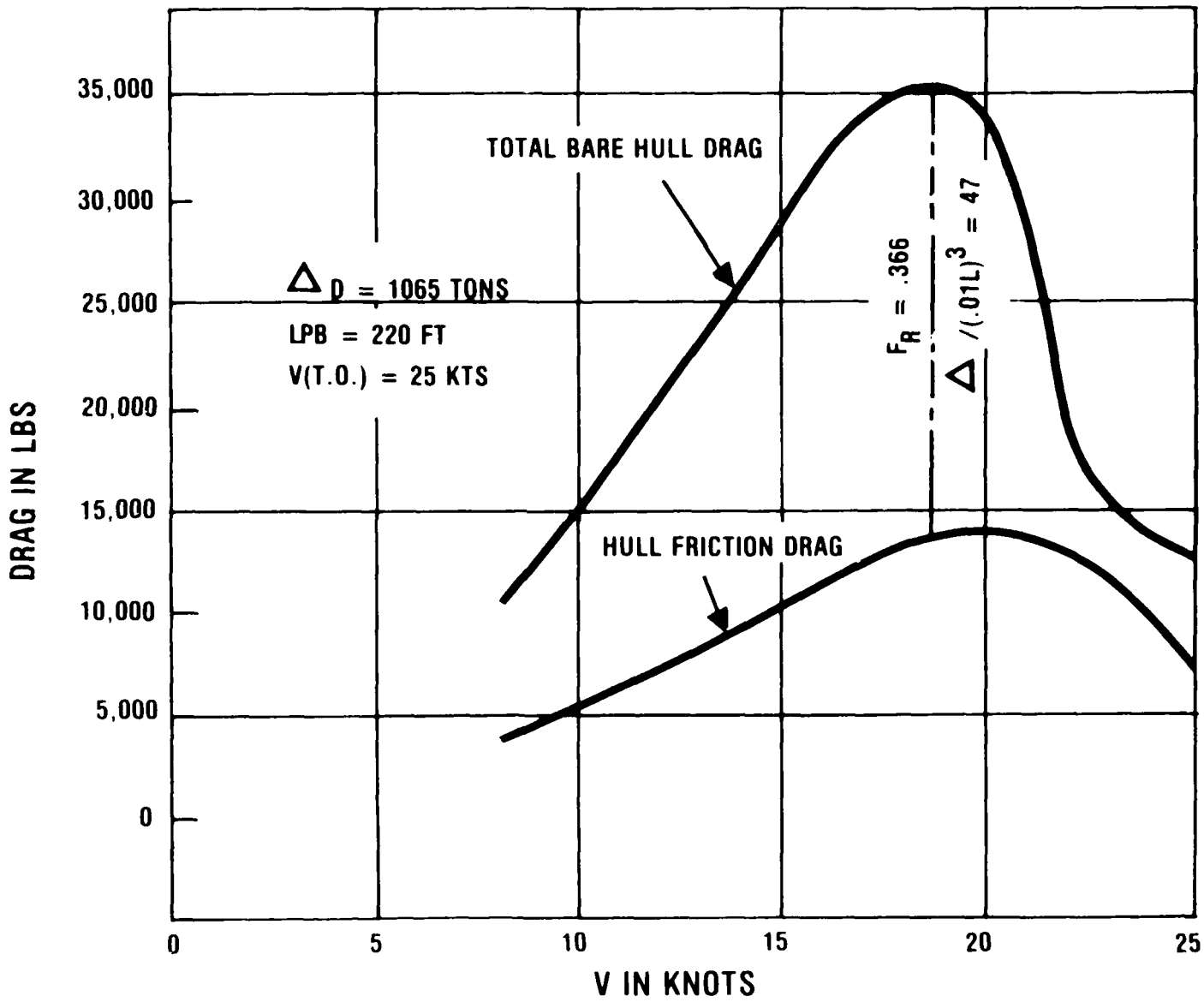

Figure 9. Bare Hull Drag for 1065-Ton, 25-Knot Takeoff Speed Design

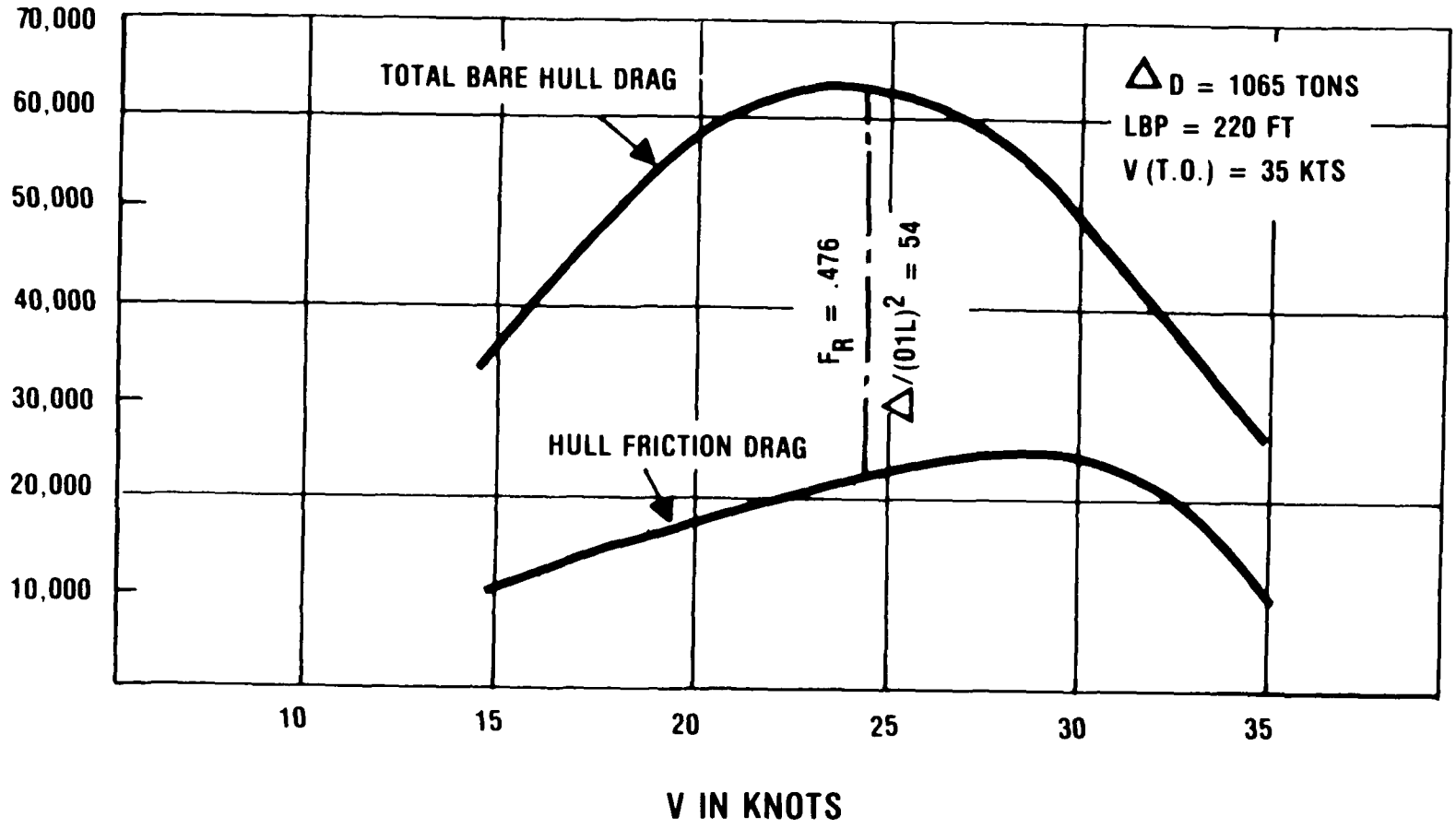

Figure 10. Bare Hull Drag for 1065-Ton, 35-Knot Takeoff Speed Design

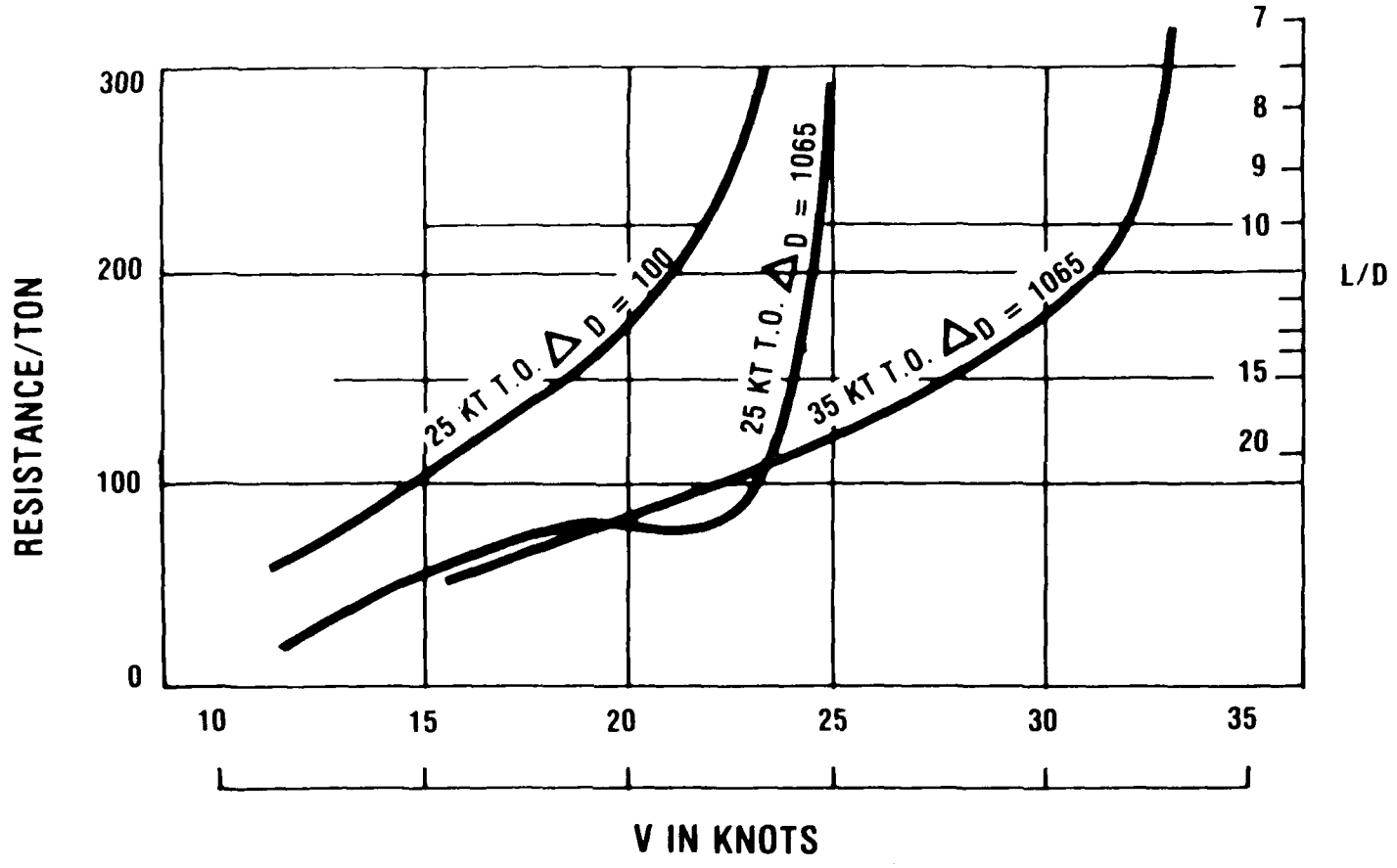

Figure 11. Bare Hull Resistance Per Unit Displacement and L/D

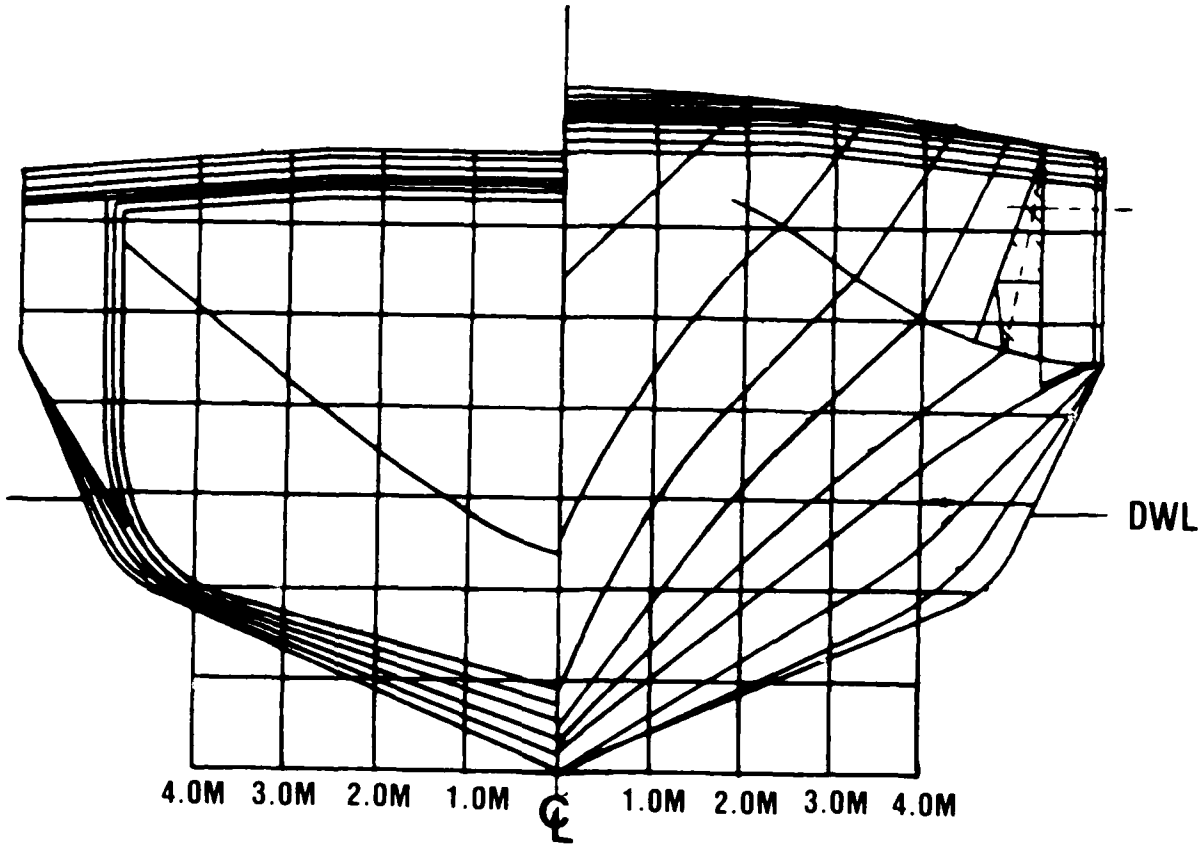

HULL PARTICULARS

LBP	56.00M	(183.7 FT)
LOA	60.20M	(197.5 FT)
BEAM AT DWL ℄	10.41M	(34.2 FT)
DRAFT AT DWL	2.90M	(9.5 FT)
DEPTH AT SIDE ℄	6.35M	(20.8 FT)
MAXIMUM BEAM	12.00M	(39.4 FT)
MAXIMUM DEPTH	7.46M	(24.5 FT)
DISPLACEMENT, FULL LOAD	786 MT	(774 LT)

Figure 12. 786-Ton ASW Hydrofoil Body Plan

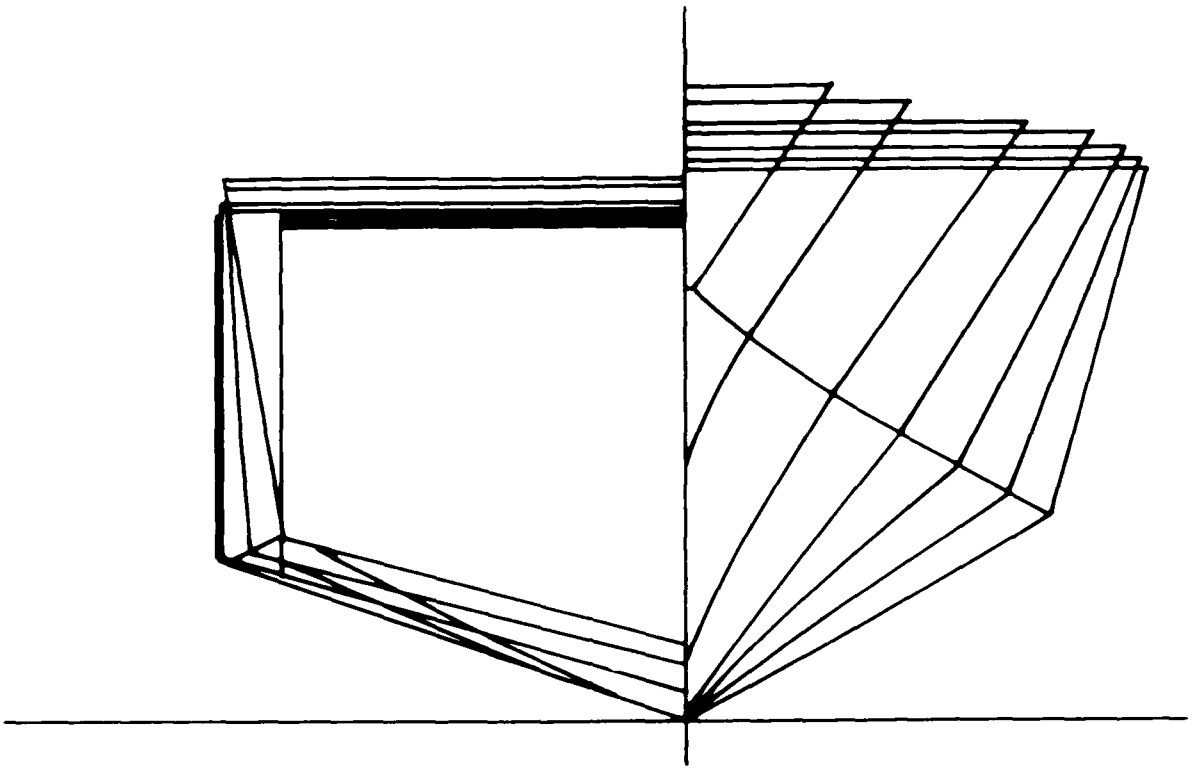

HULL PARTICULARS

LBP	44.66M (146.5 FT)
LOA	48.78M (160.0 FT)
BEAM AT DWL ⋈	9.70M (31.8 FT)
DRAFT AT DWL	2.53M (8.3 FT)
DEPTH AT SIDE ⋈	5.55M (18.2 FT)
MAXIMUM BEAM	10.67M (35.0 FT)
DISPLACEMENT, FULL LOAD	511 MT (503 LT)

Figure 13. PCM Body Plan

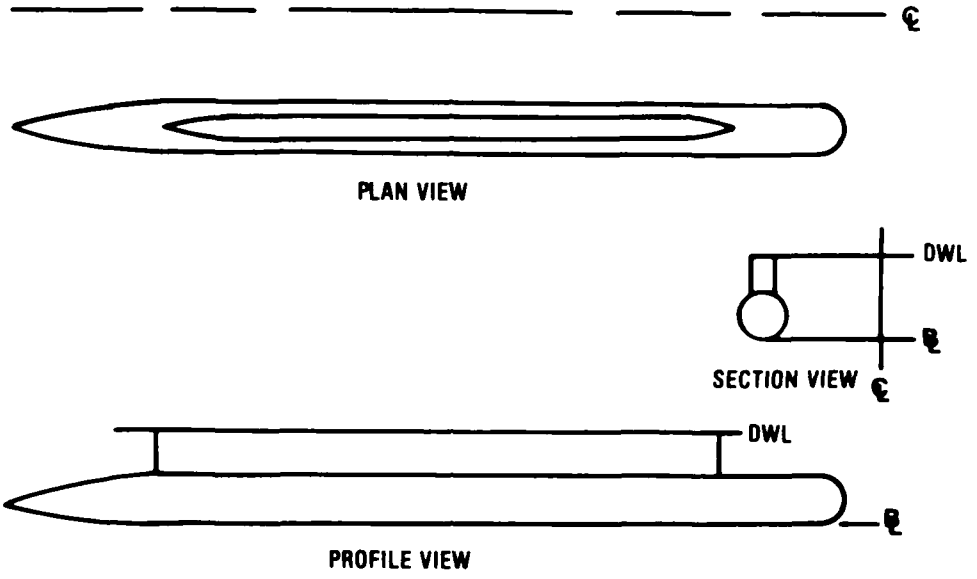

Figure 14A. Historical Frigate

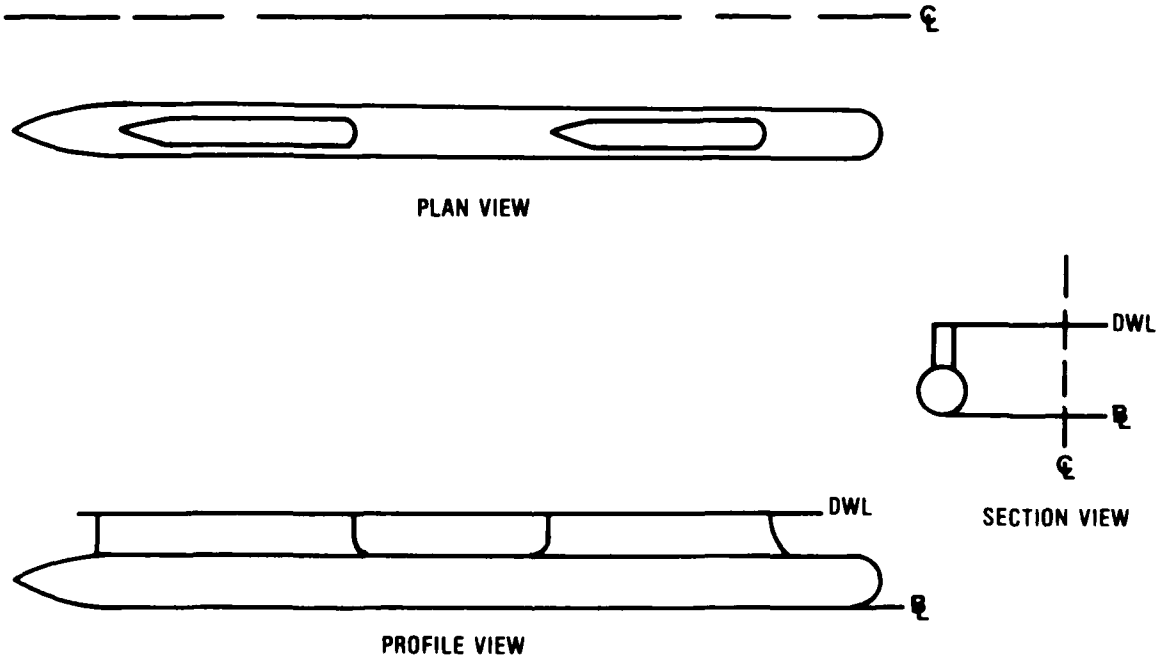

Figure 14B. Historical Frigate

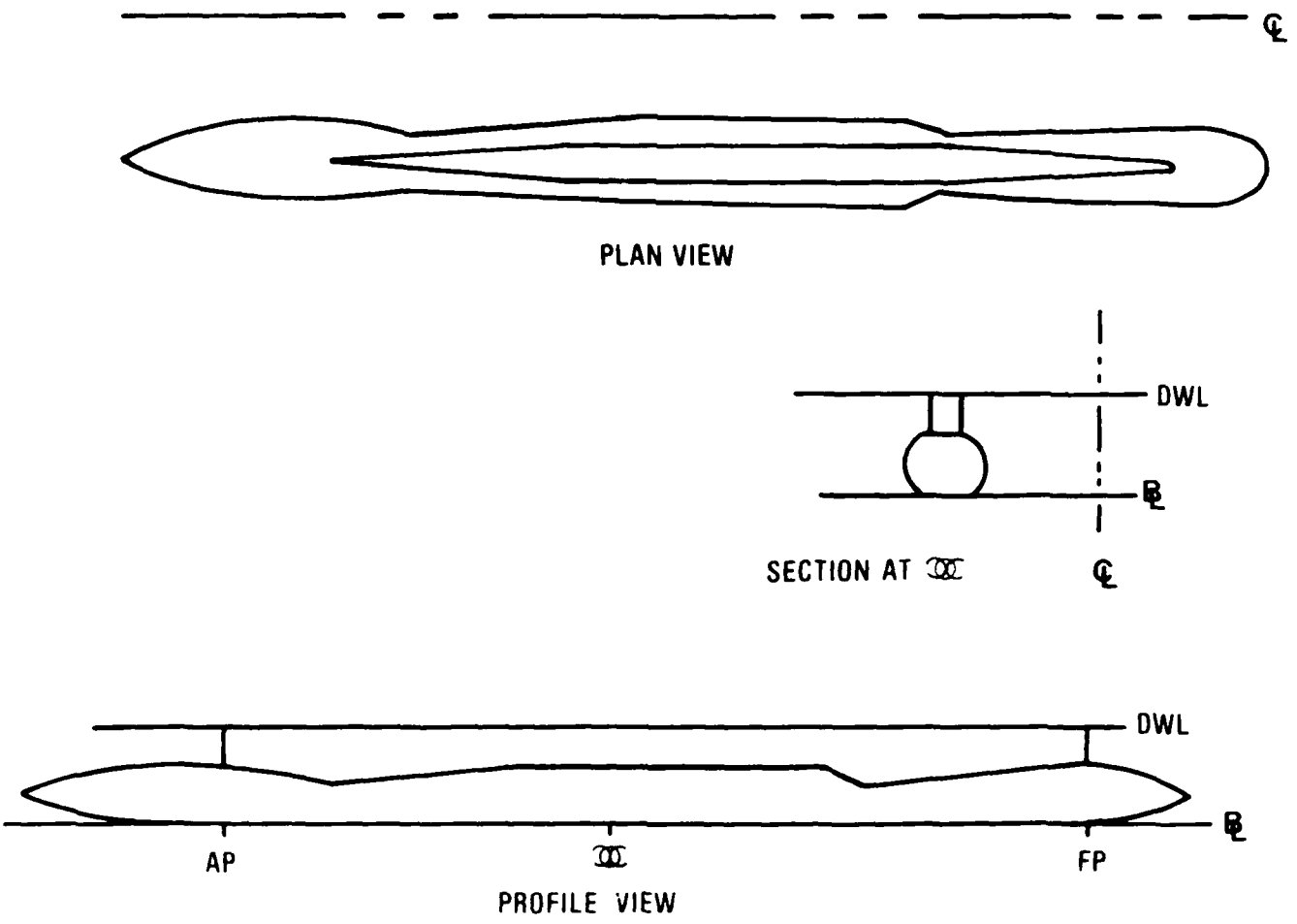

Figure 15. Current Frigate

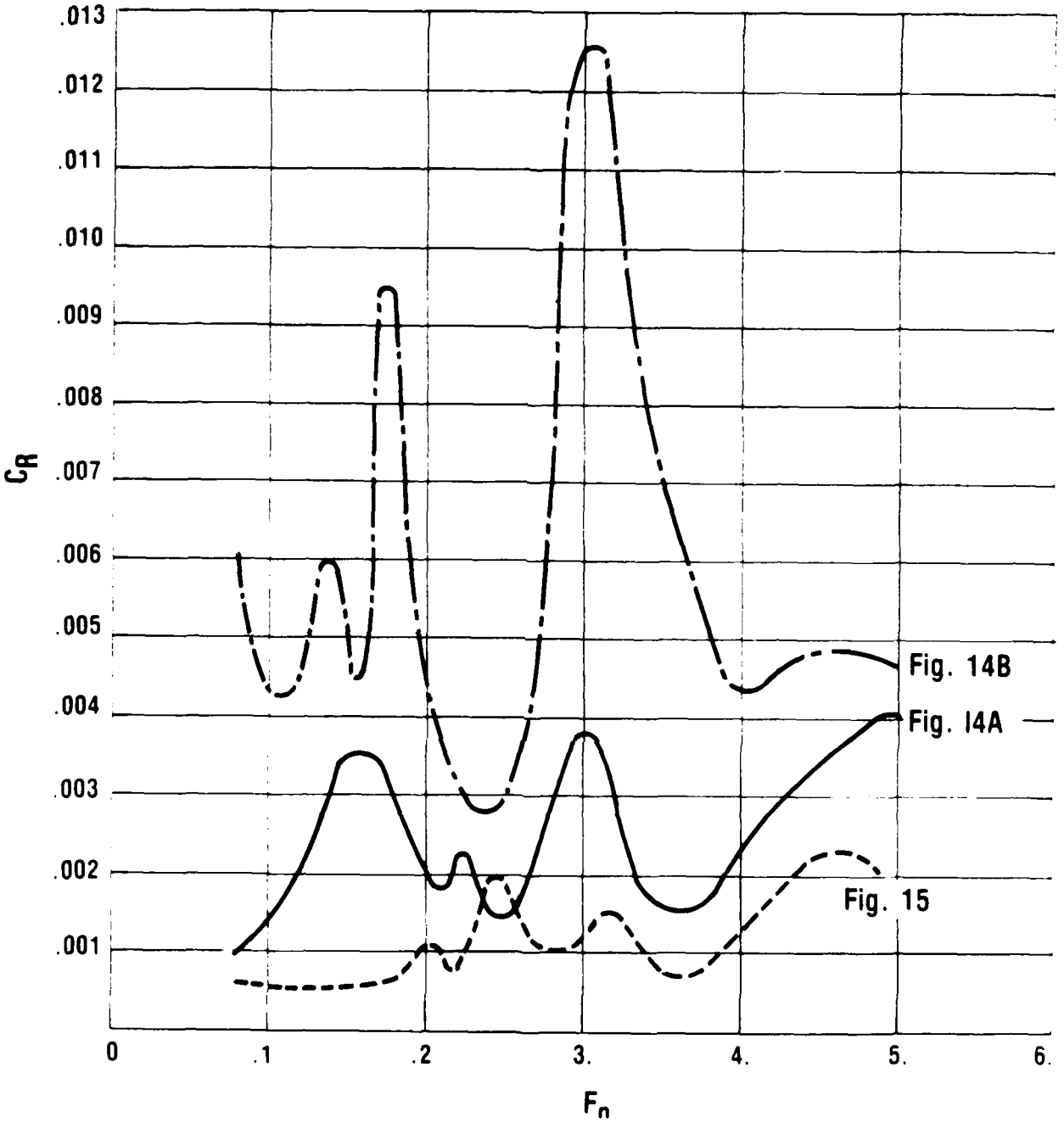

Figure 16. Residuary Resistance vs. Froude Number

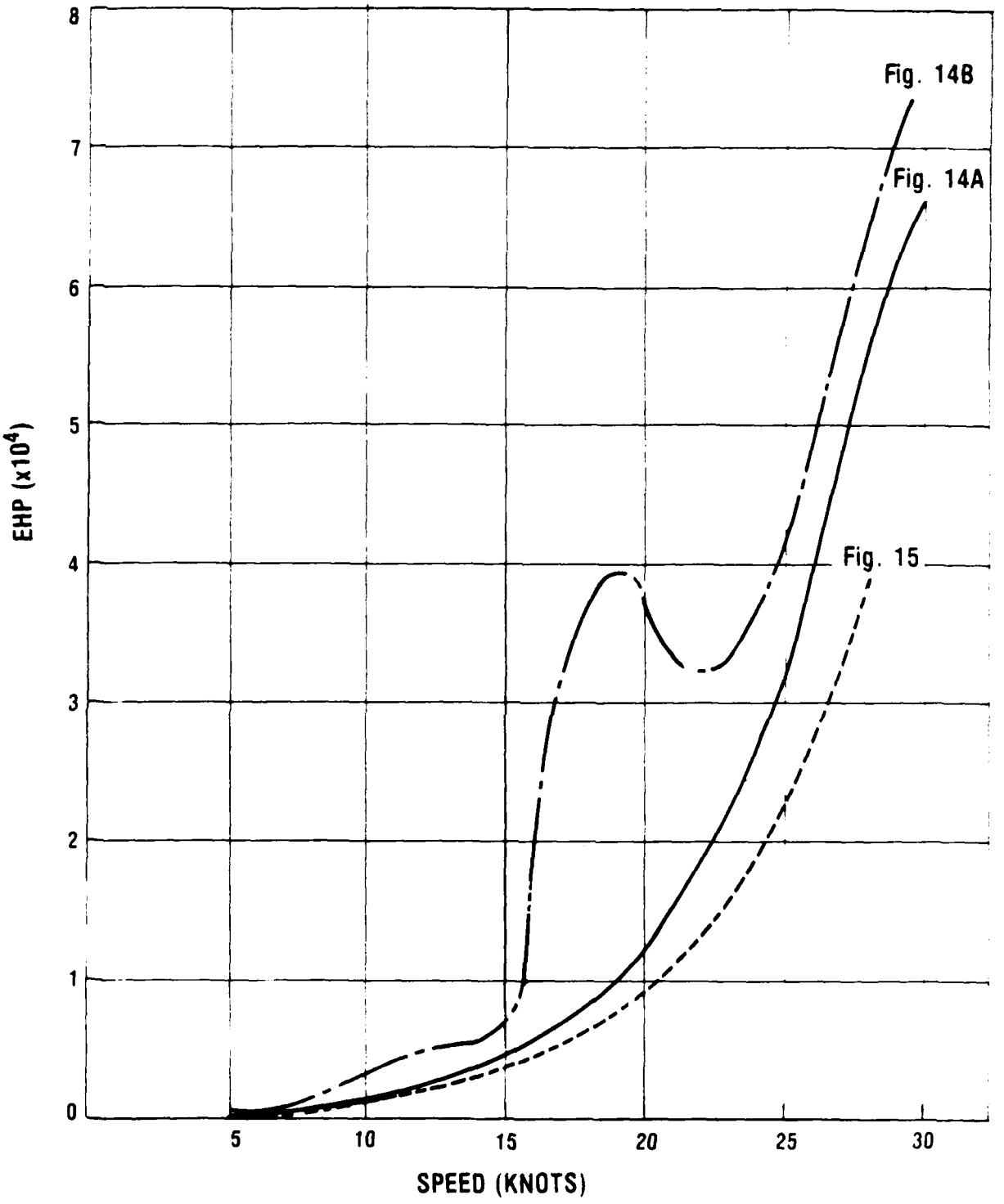

Figure 17. Effective Horsepower vs. Speed

Figure 18. Hovercraft Development Limited Test Craft D.1

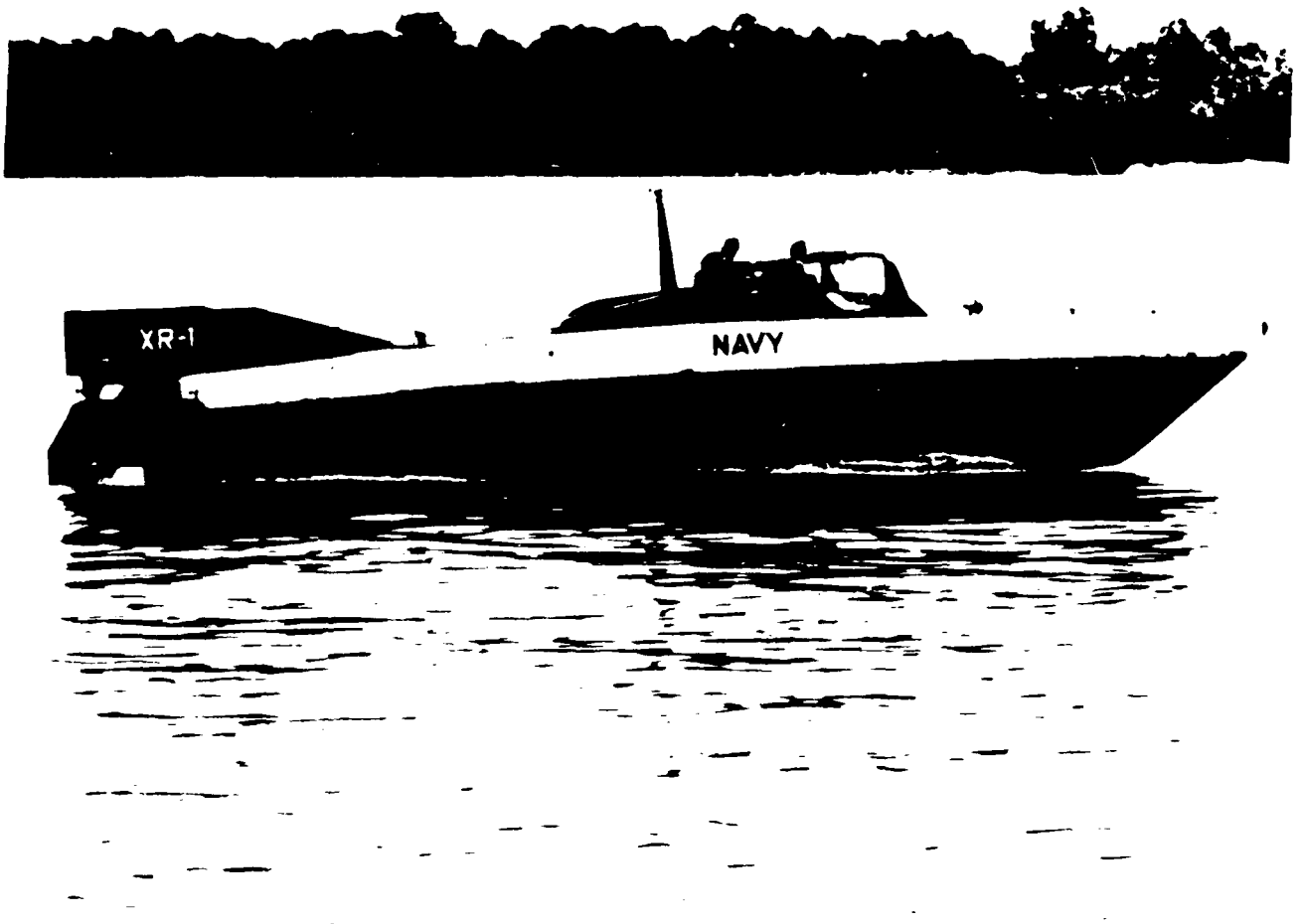

Figure 19. XR-1

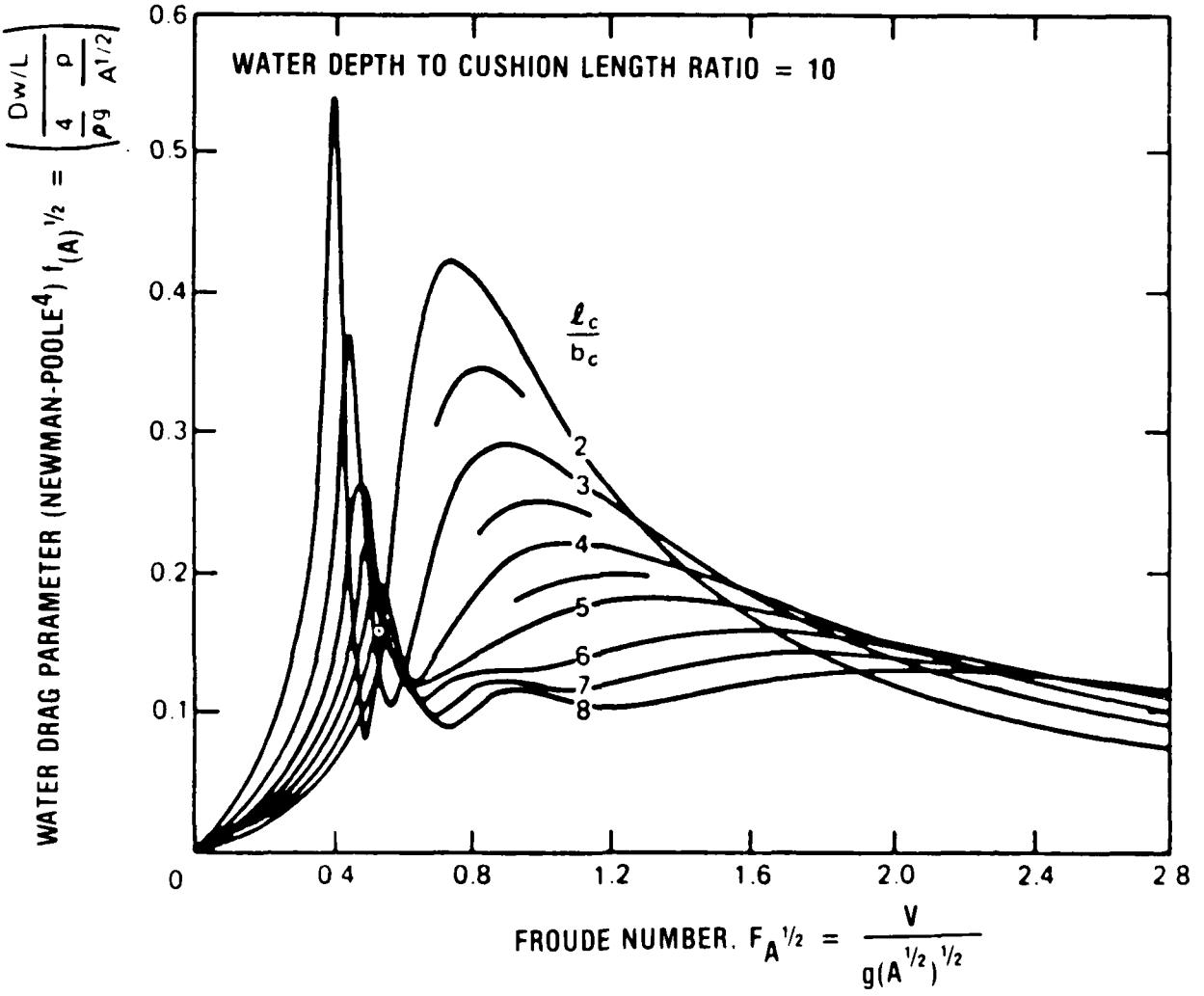

Figure 20. Wave Drag Parameter Based on $A^{\frac{1}{2}}$ vs. Froude Number Based on $A^{\frac{1}{2}}$

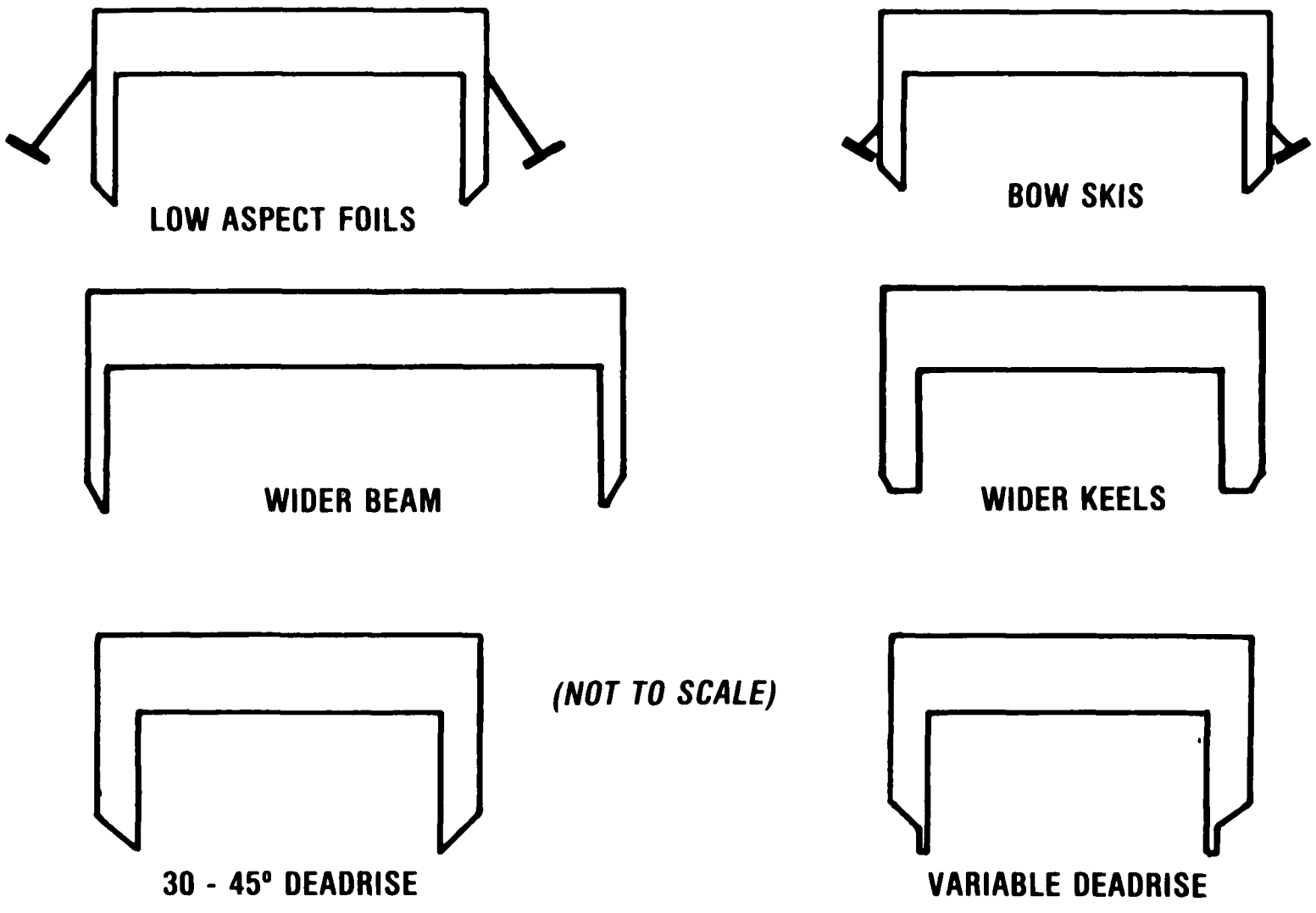

Figure 21. Dynamic Stability Control Concepts

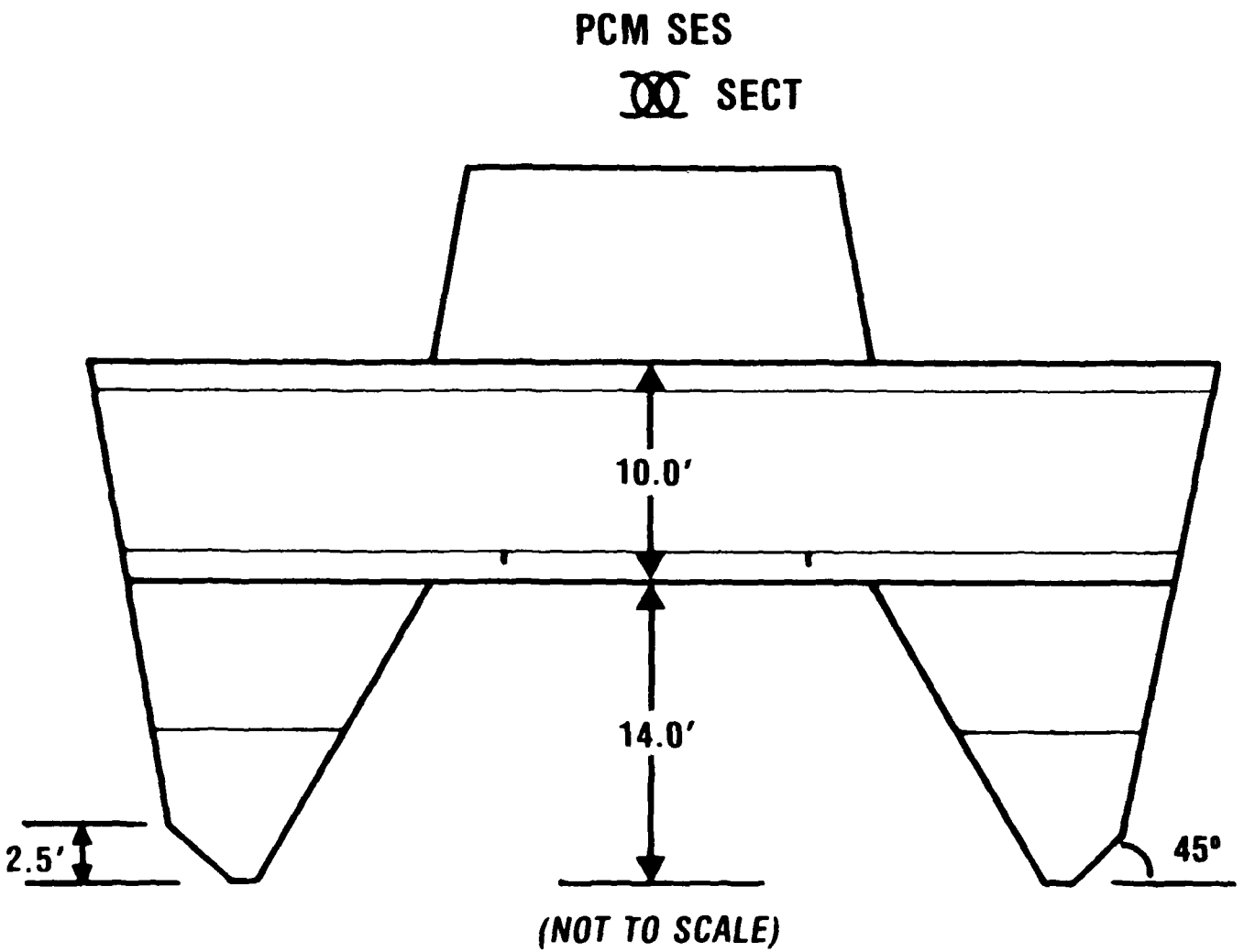

Figure 22. PCM SES Cross Section

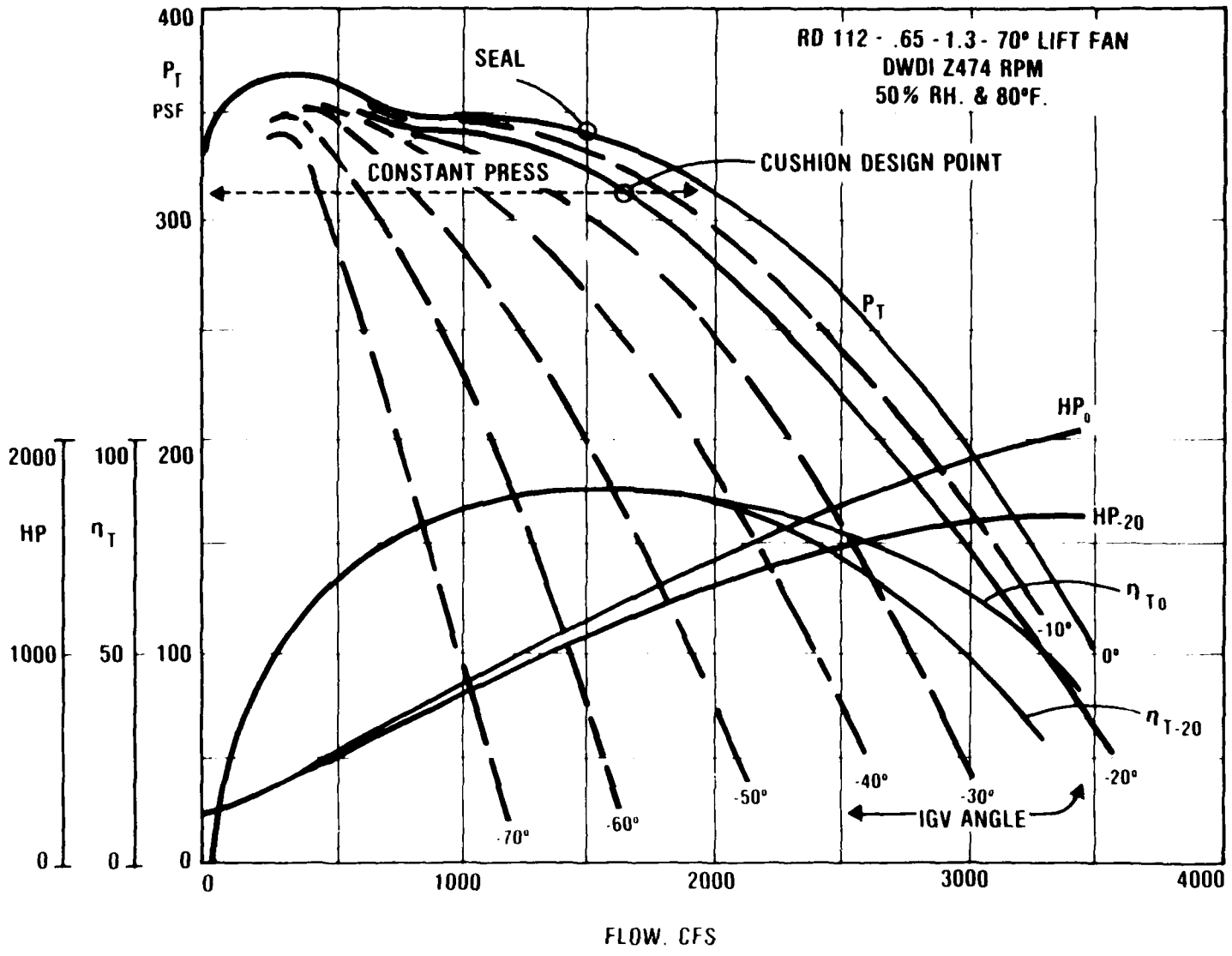

Figure 23. Constant Pressure, Variable Flow Lift Fans

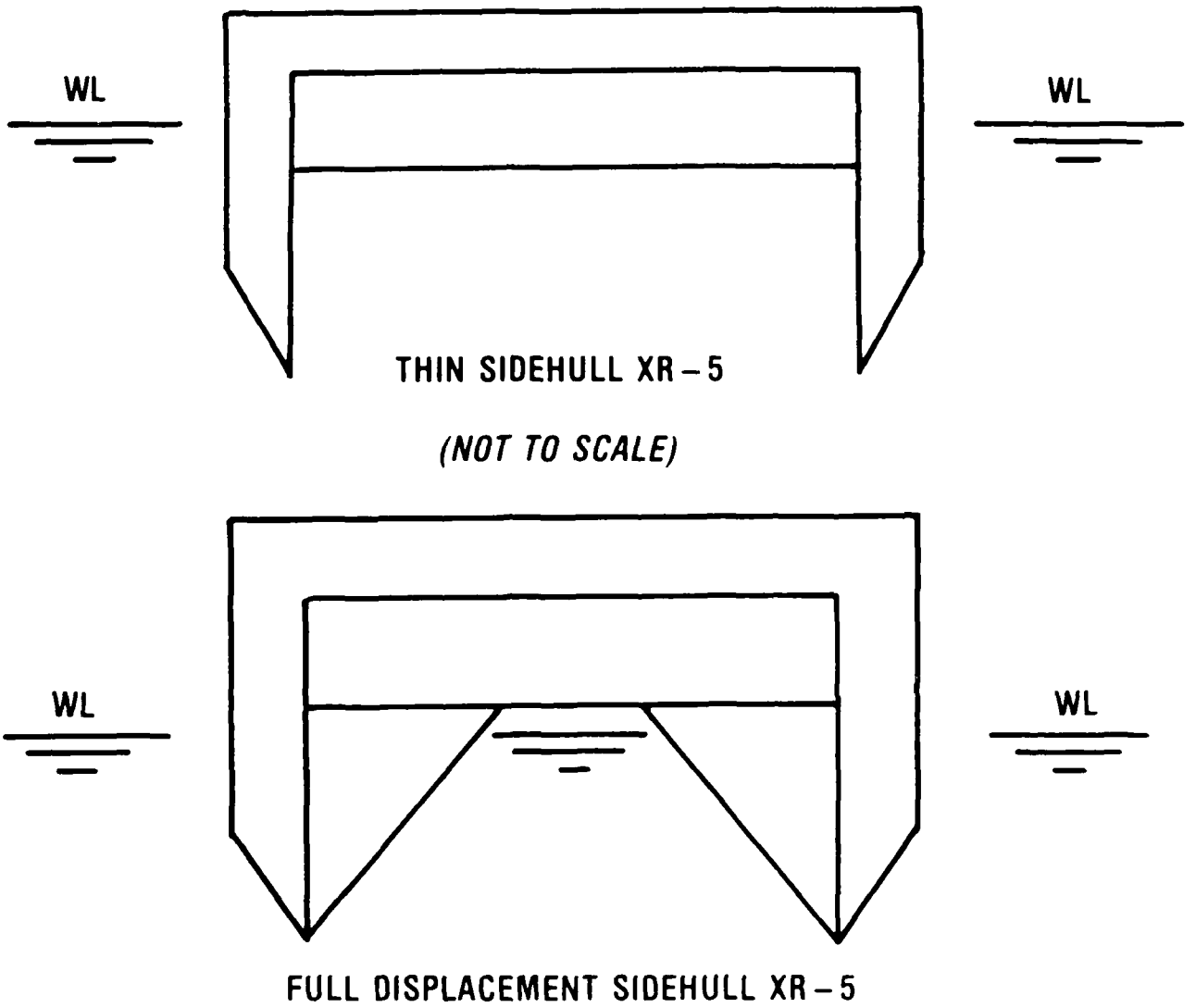

Figure 24. Thin and Full Displacement Sidehulls

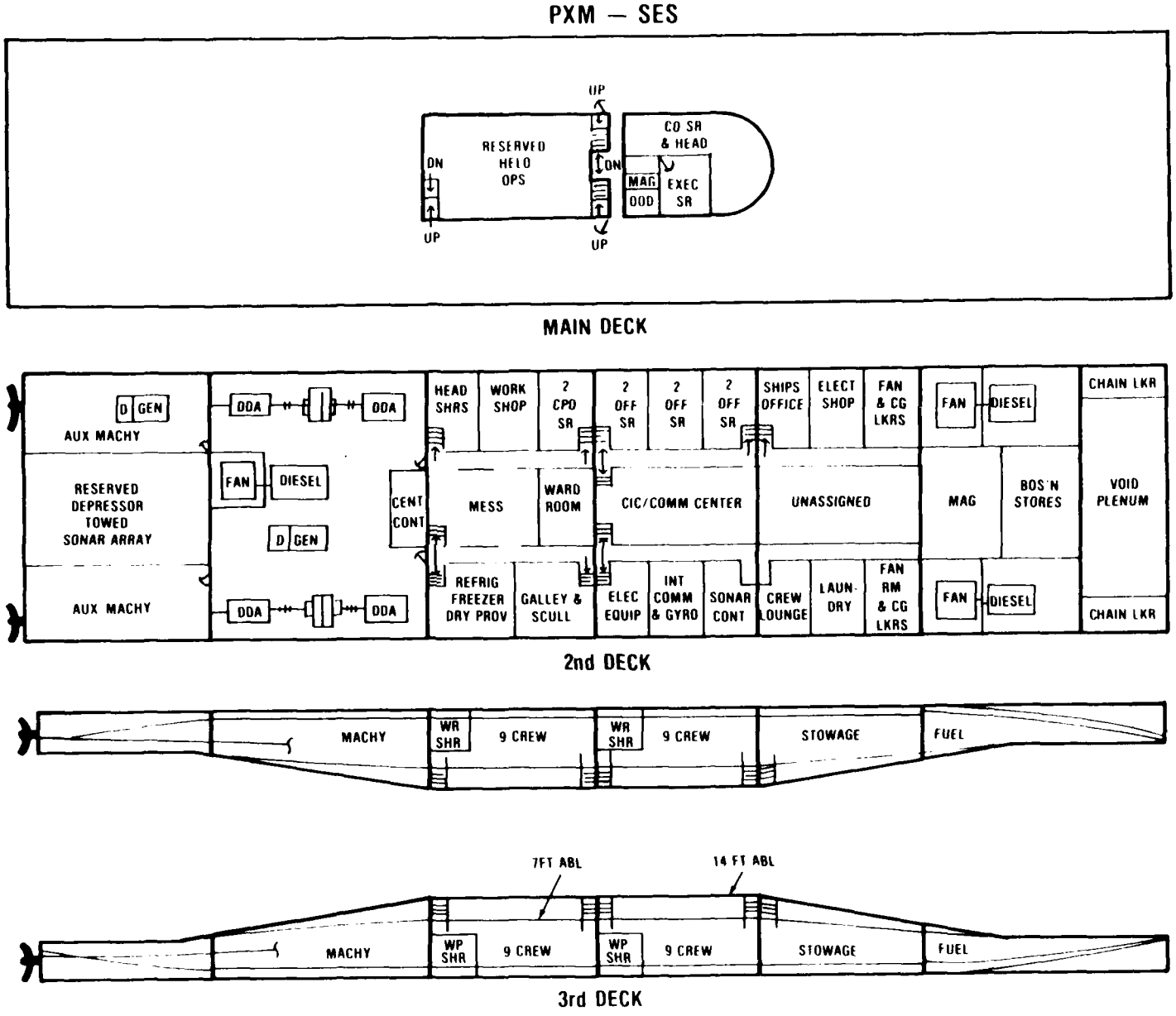

Figure 25. PCM Hull Configuration

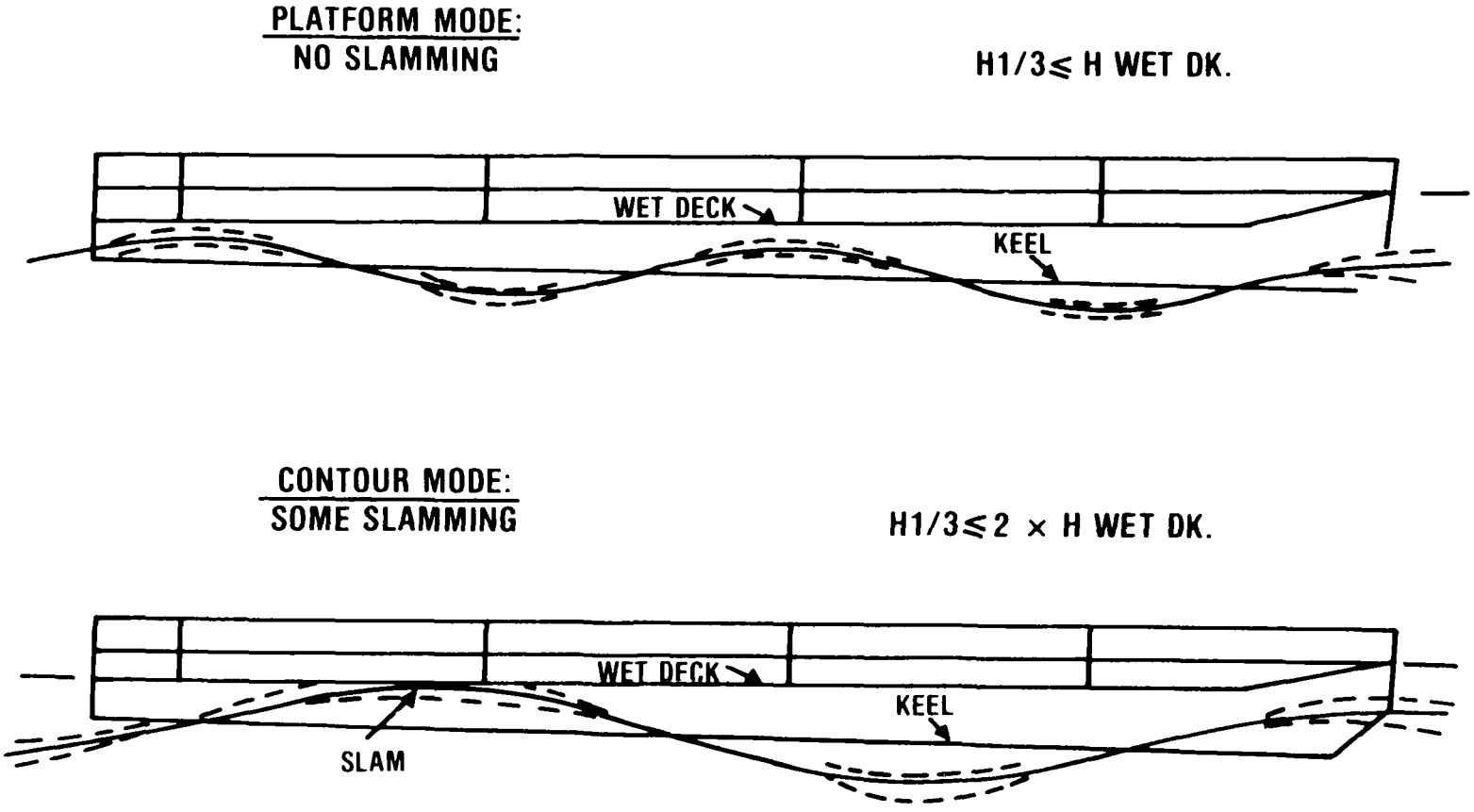

Figure 26. PCM Sea State vs. Wet Deck Slamming (On-Cushion)

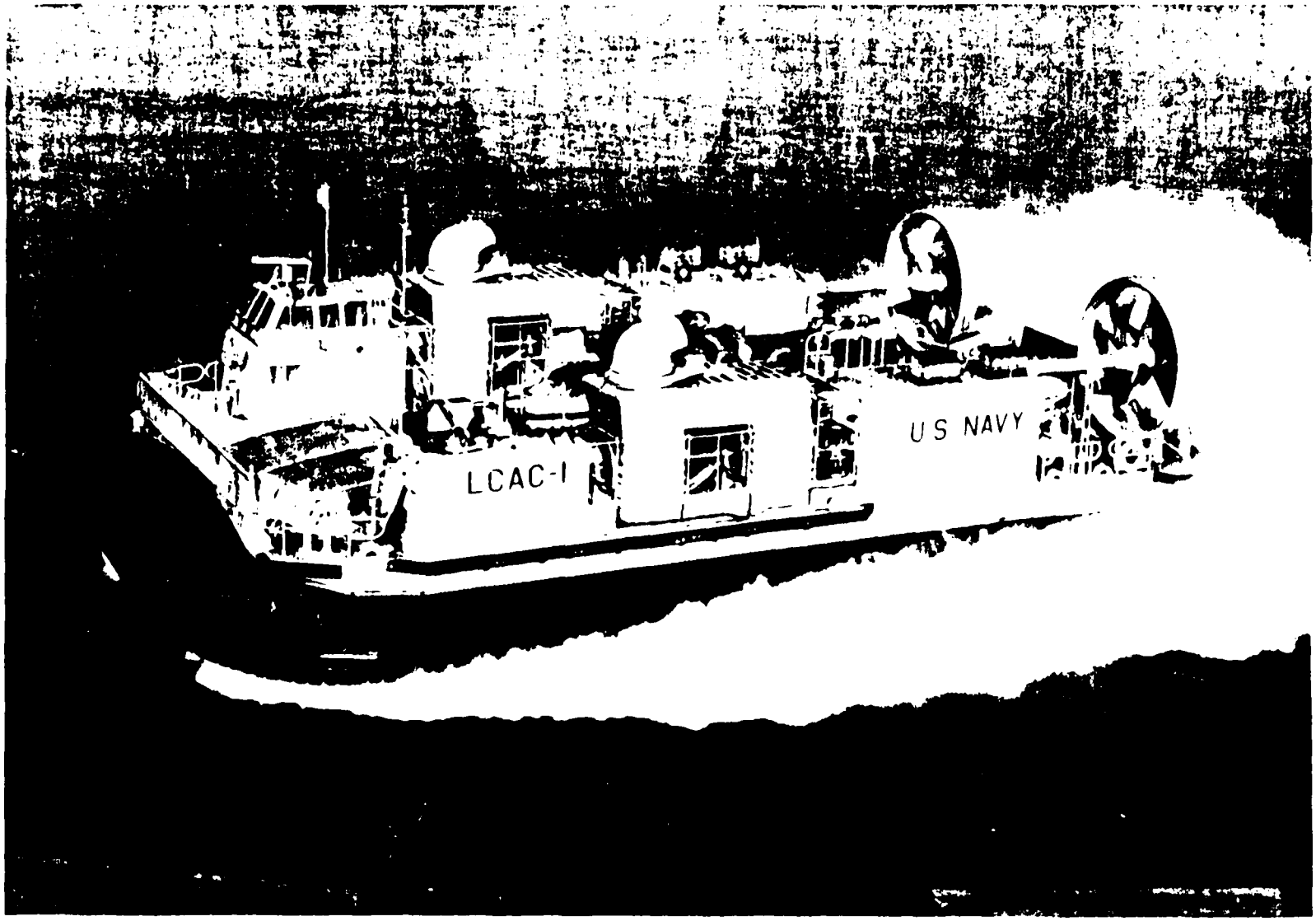

Figure 27. U.S. Navy's LCAC-001

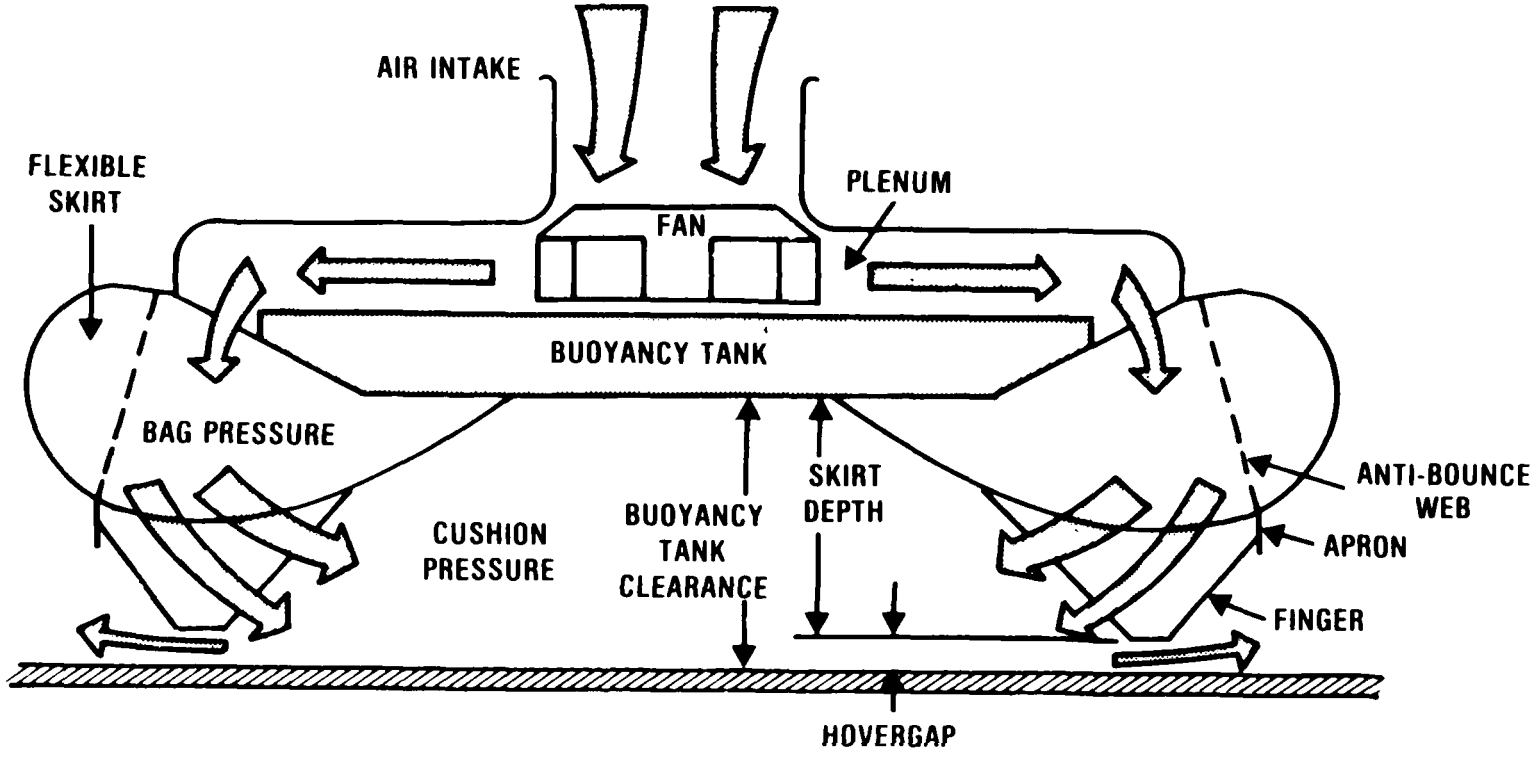

Figure 28. Illustration of Airflow Through an ACV

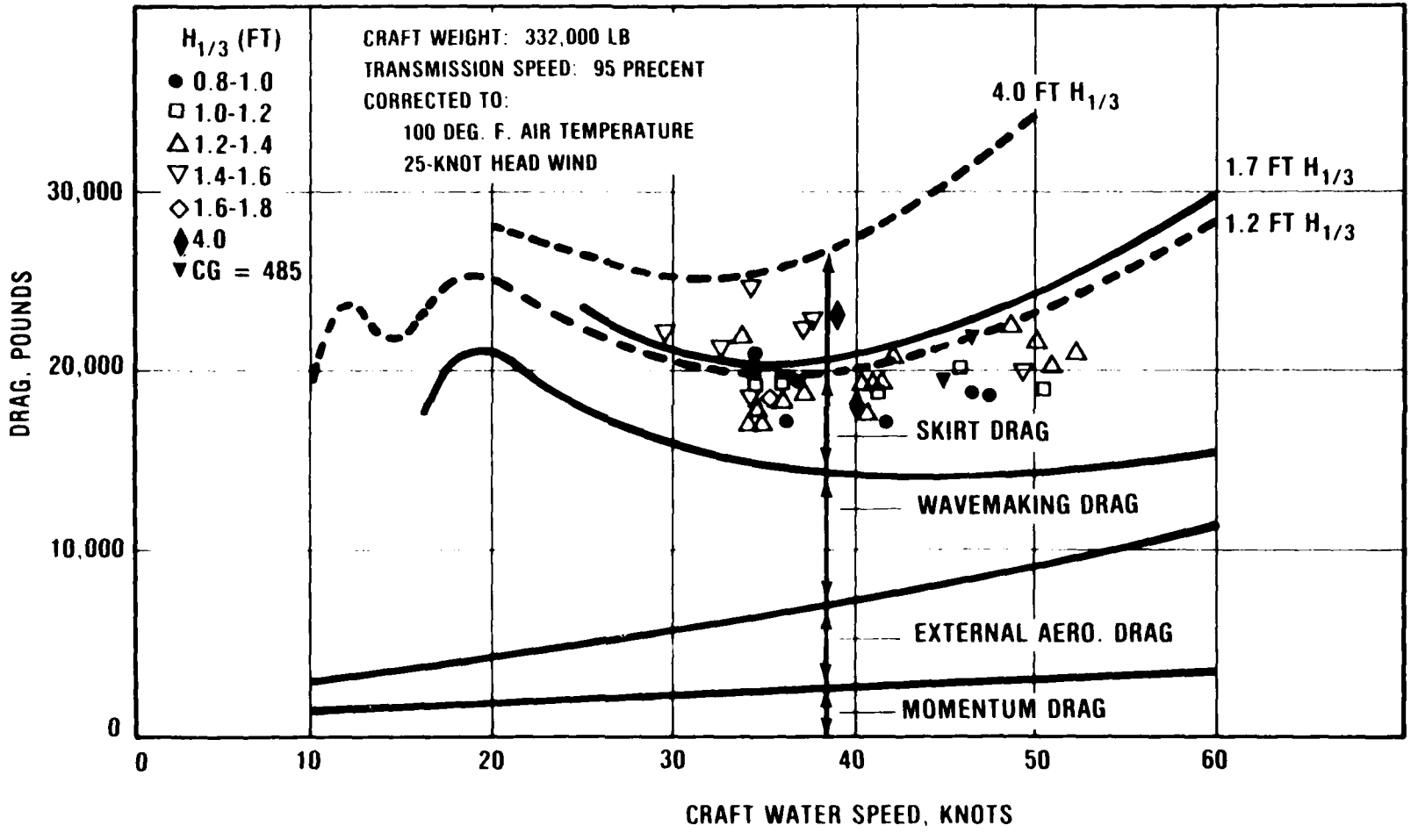

Figure 29. JEFF(B) Drag Overwater

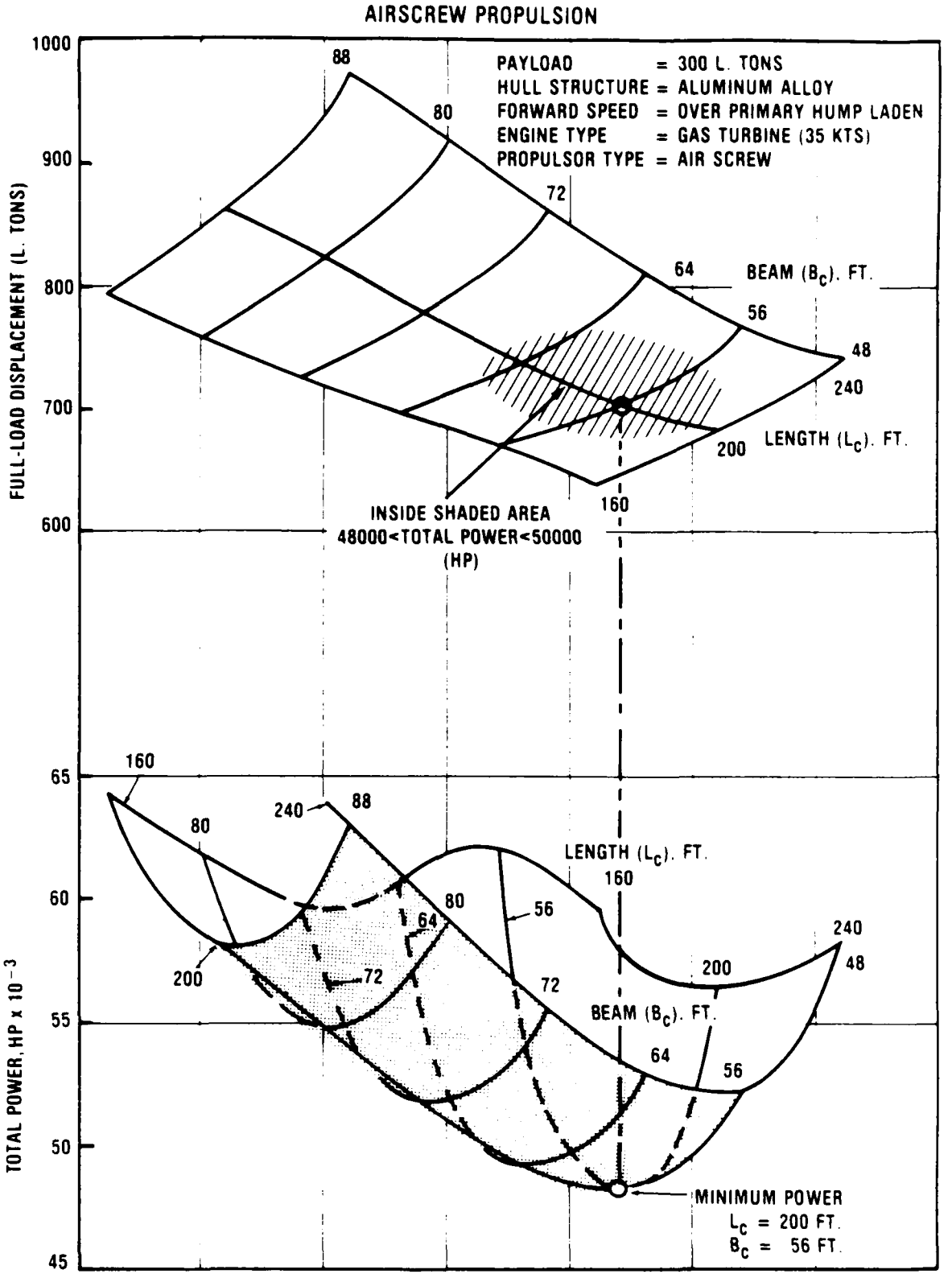

Figure 30. Variation of Full-Load Displacement and Total Power with Hull Length and Beam for an ACV (Aluminum Hull, Gas-turbine Engine, Airscrew, 300 L. Ton Payload)

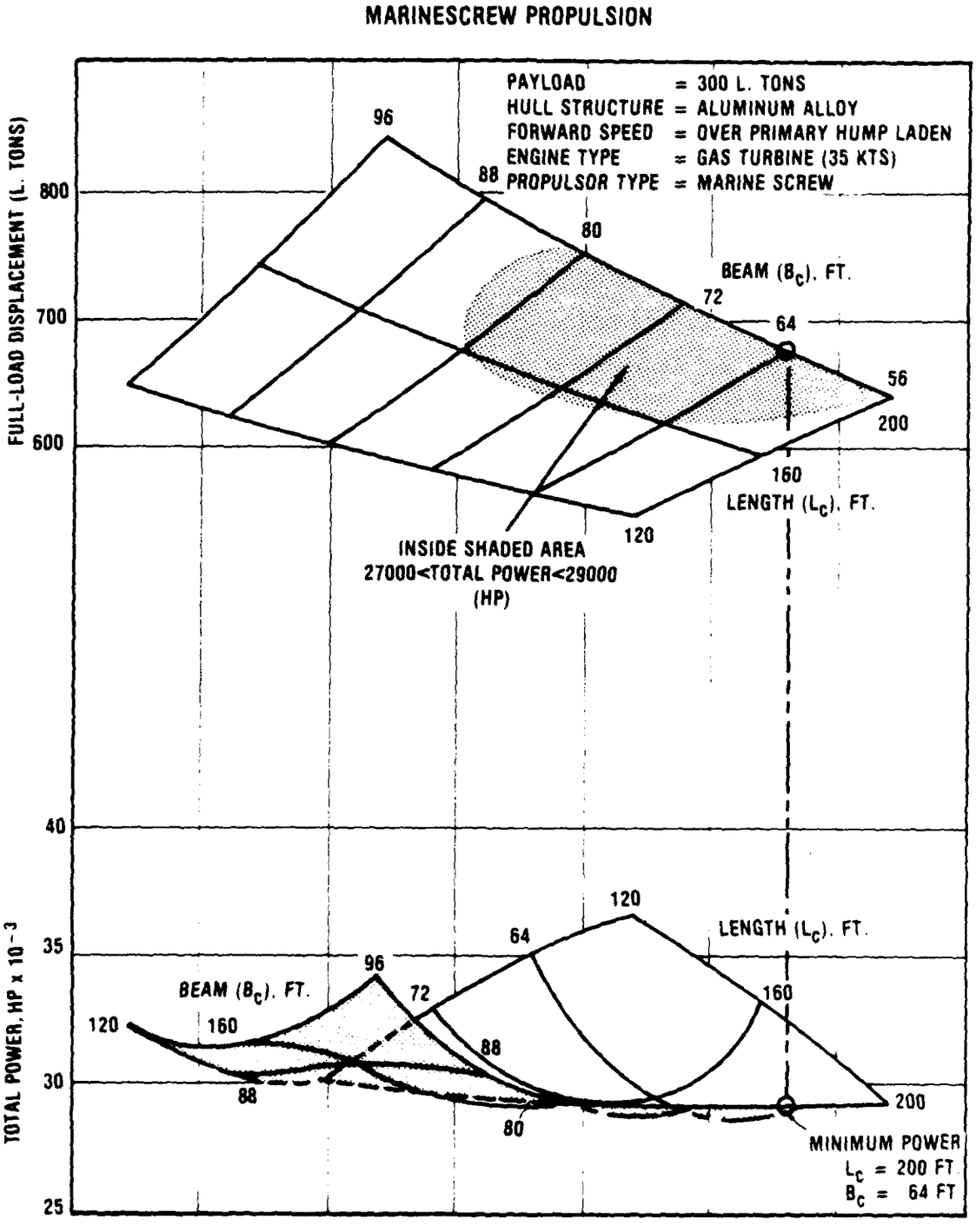

Figure 31. Variation of Full-Load Displacement and Total Power with Hull Length and Beam for an ACV (Aluminum Hull, Gas-turbine Engine, Marine Screw, 300 L. Ton Payload)

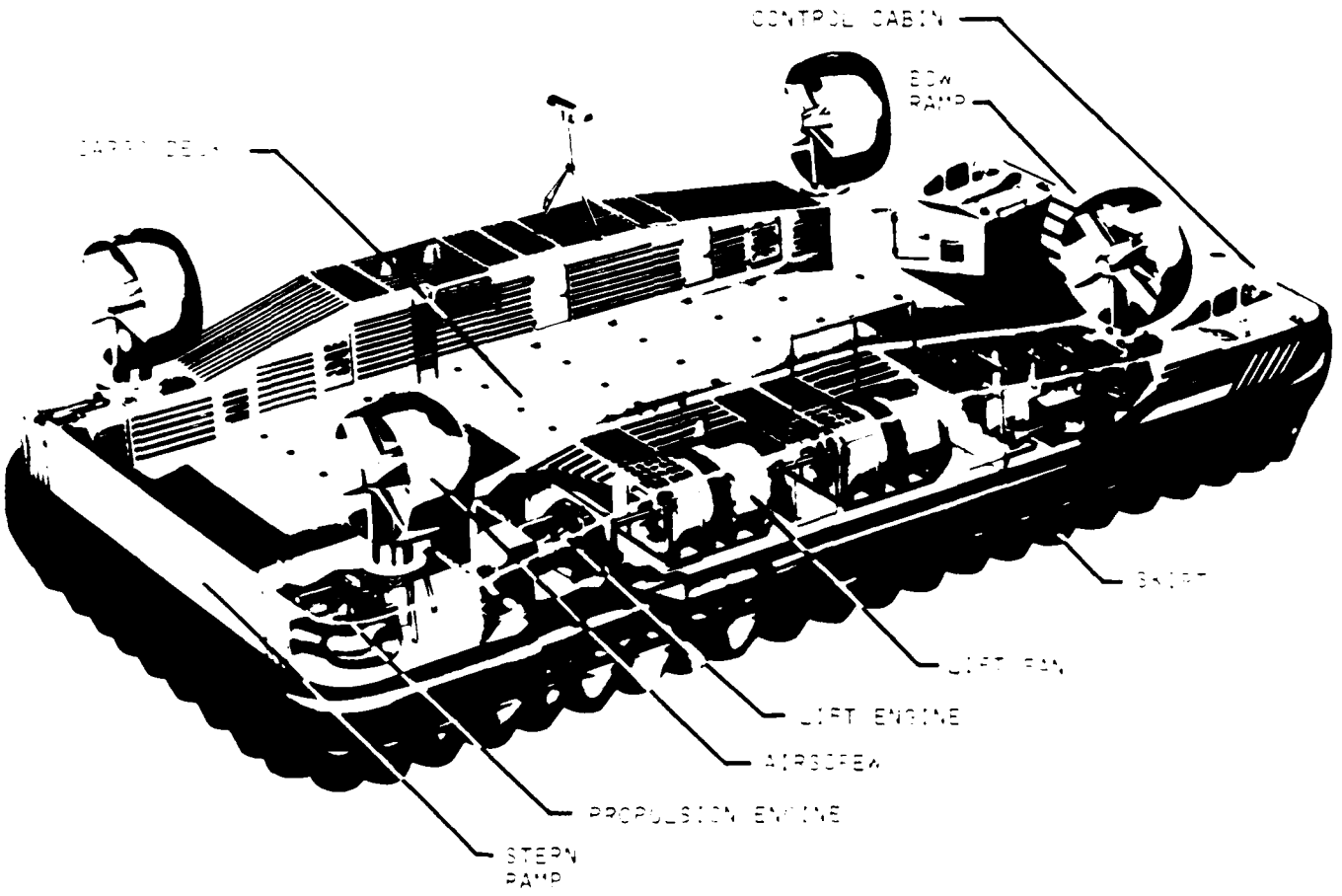

Figure 32. Illustration of U.S. Navy's AALC JEFF(A)

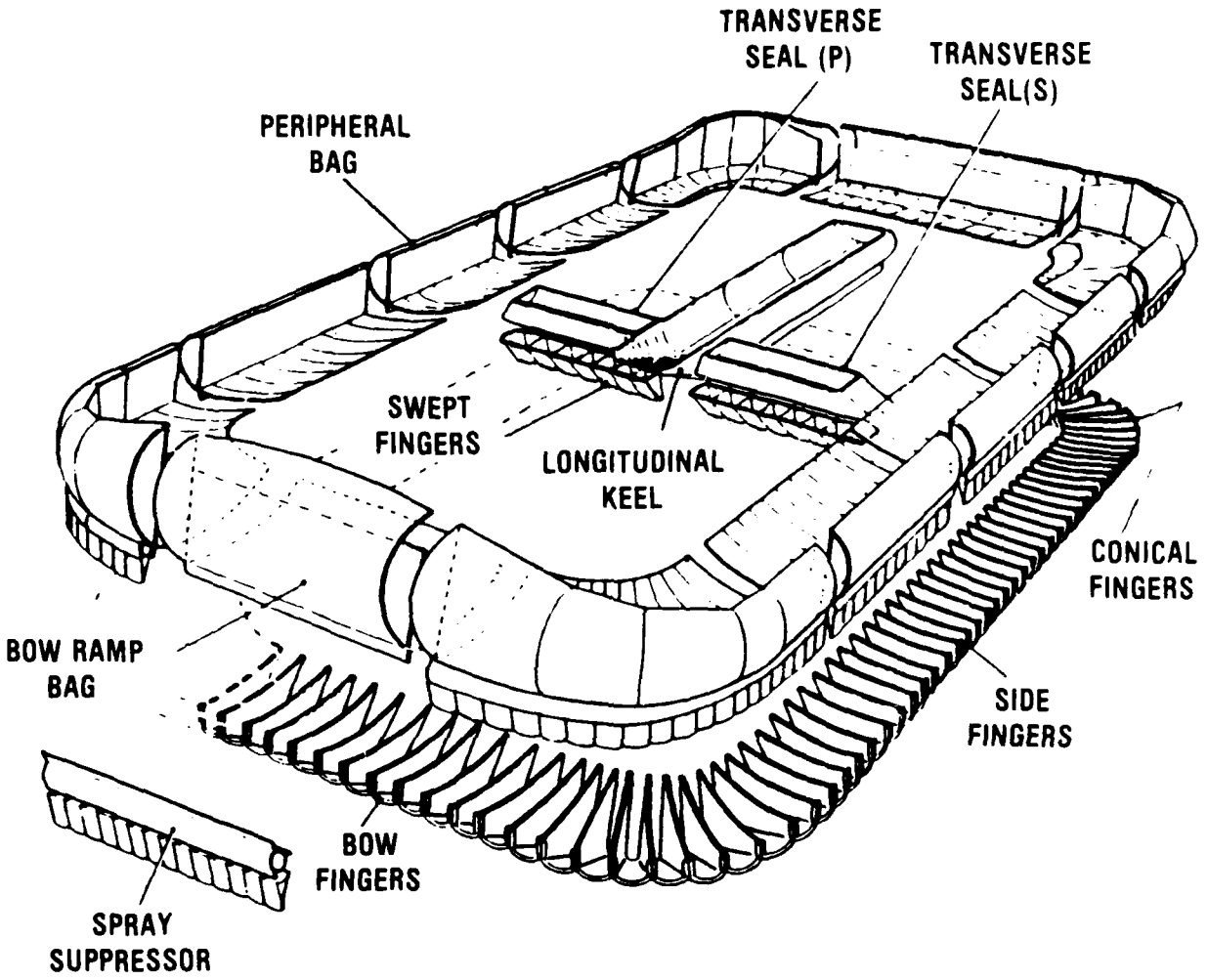

Figure 33. Major Elements of Bag/Finger Skirt

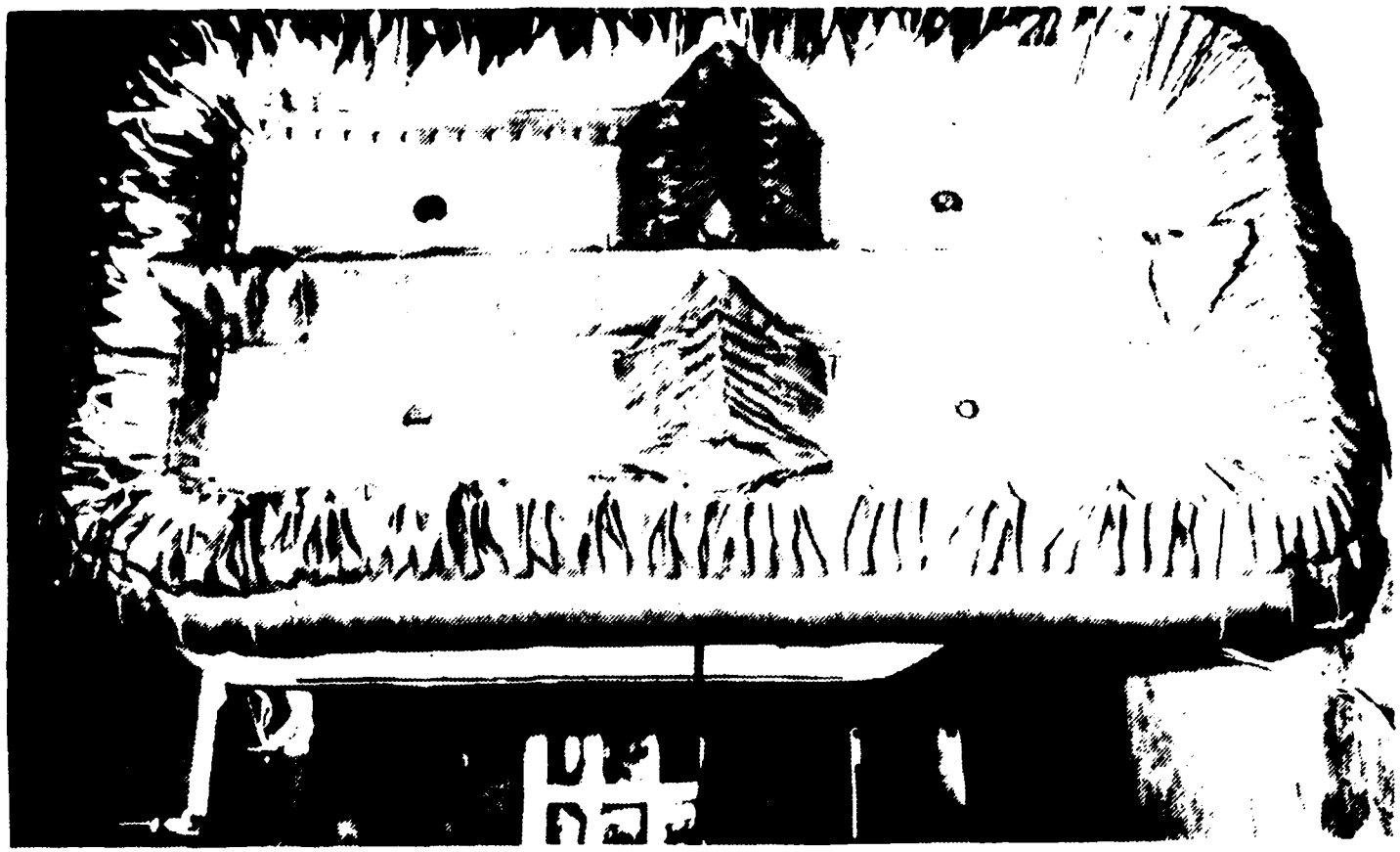

Figure 34. ACV Model with Bag/Finger Skirt as Used on AALC JEFF(B)

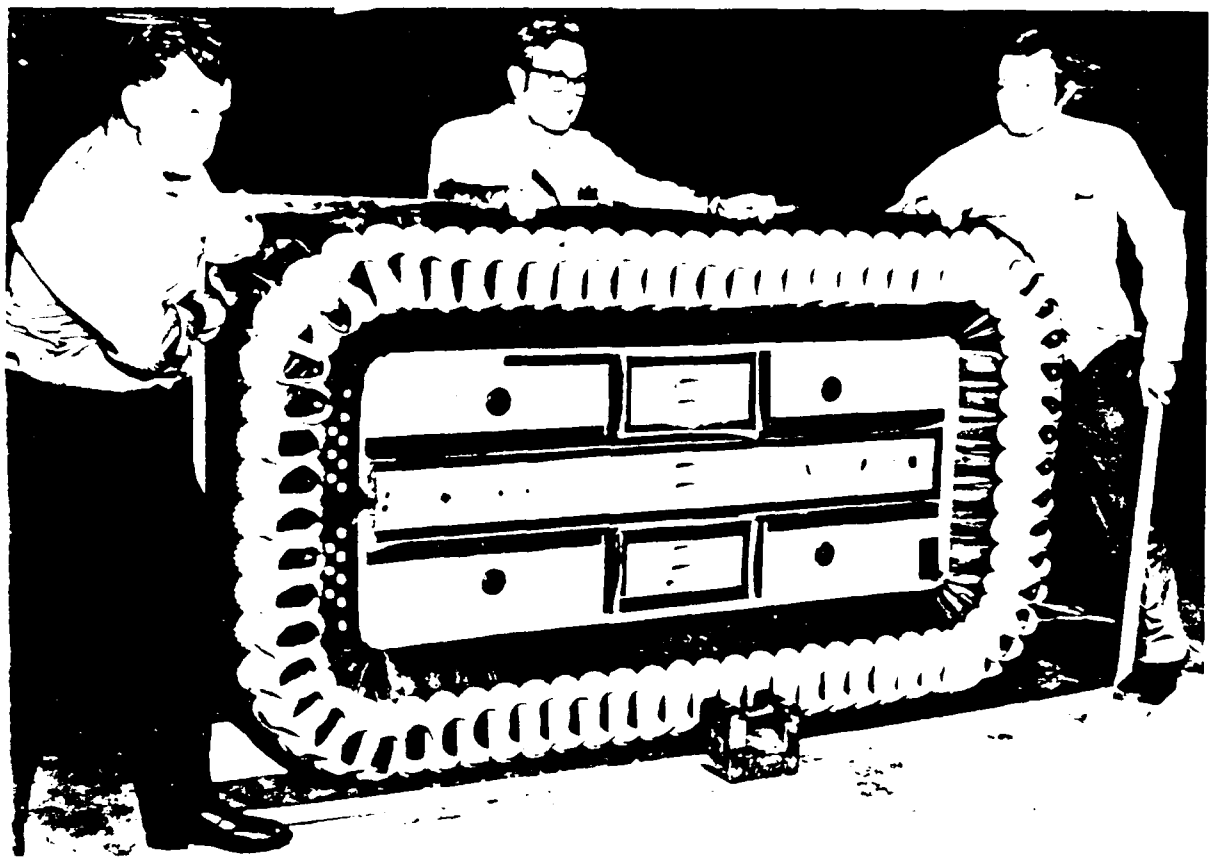

Figure 35. ACV Model with Loop-Pericell Skirt Similiar to That Used on AALC JEFF(A)

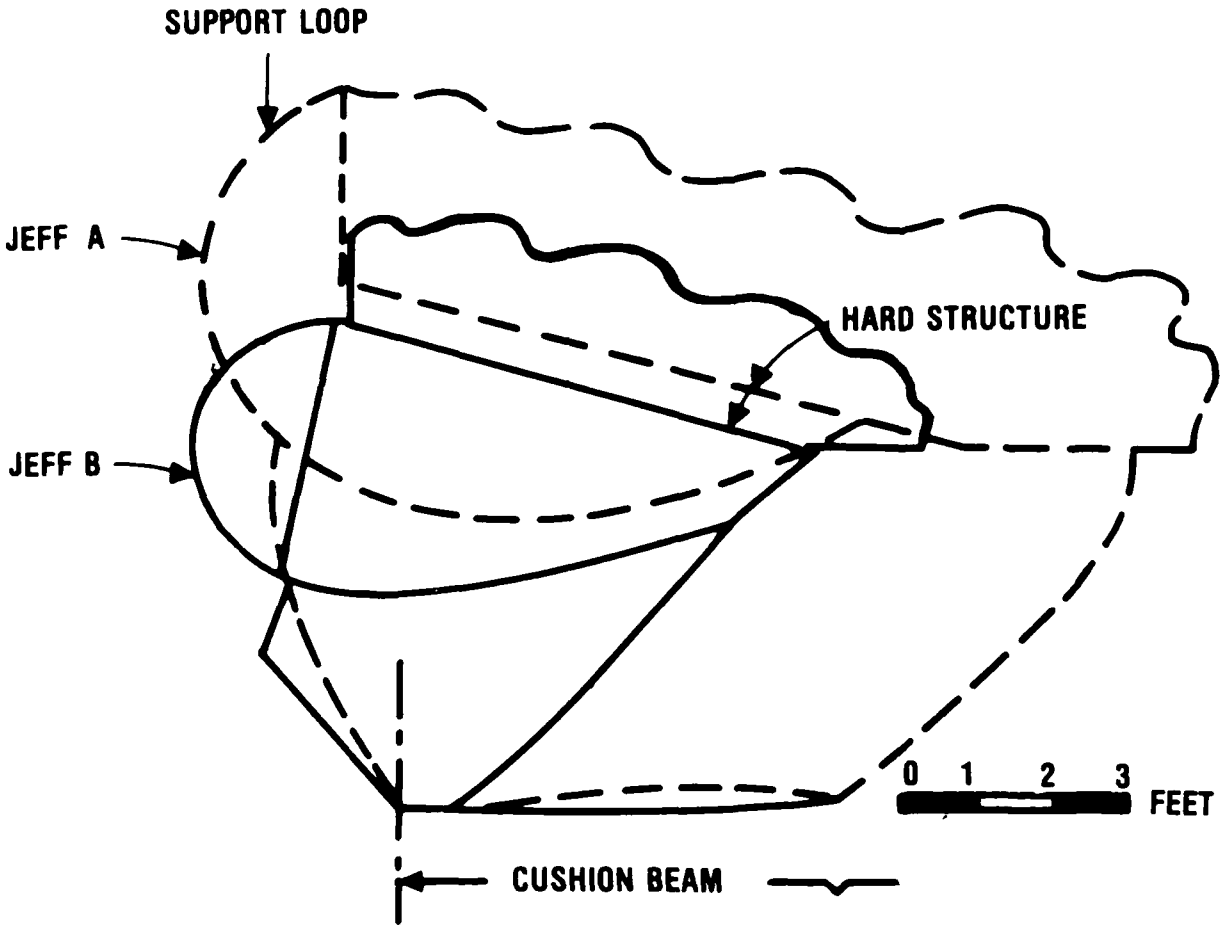

Figure 36. Comparison of JEFF Craft Side Skirt Sections

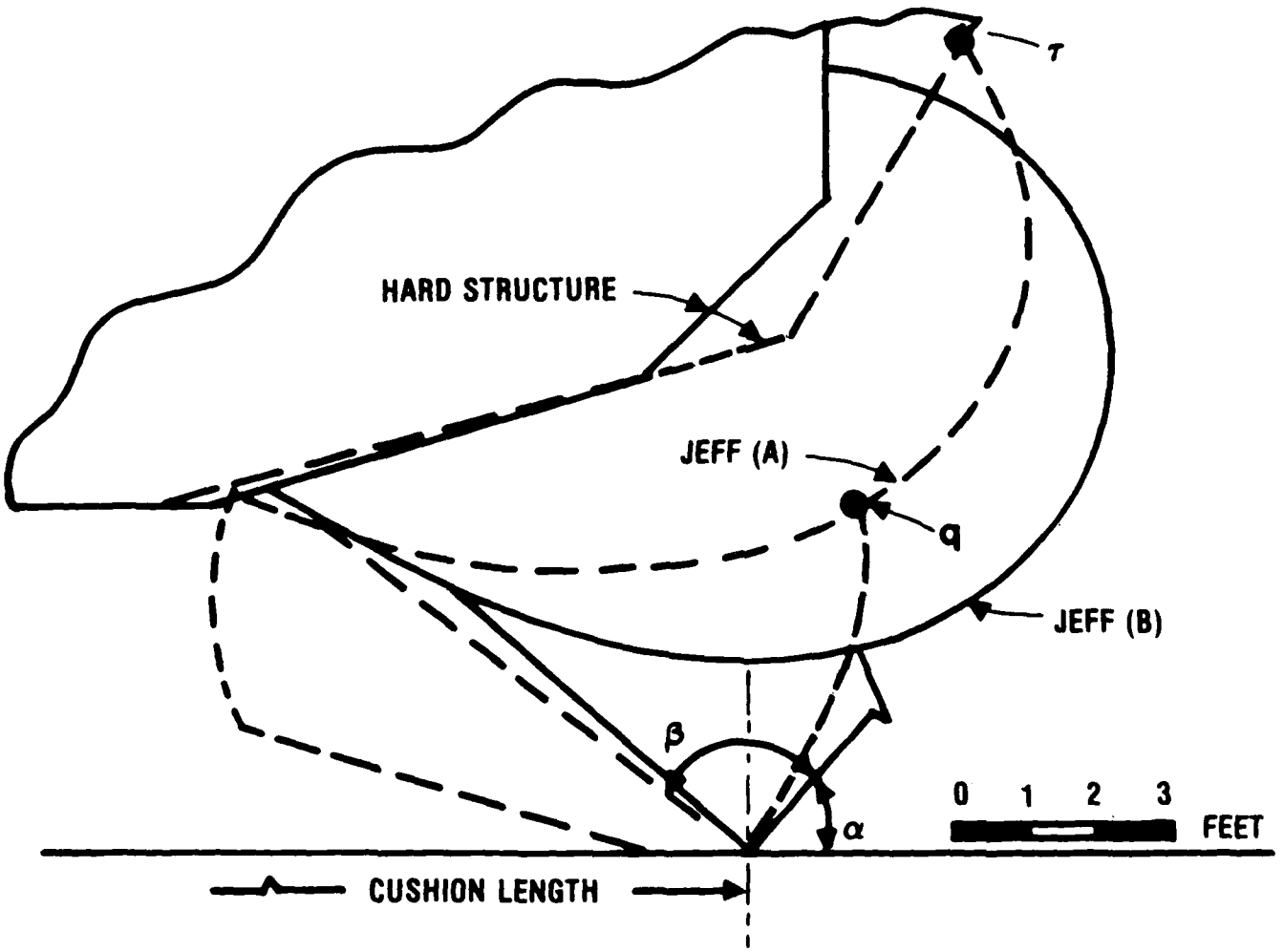

Figure 37. Comparison of JEFF Craft Bow Skirt Sections

END

12-86

DTIC